Title

Mass independent sulfur isotope signatures in CMs: Implications for sulfur chemistry in the early solar system

Authors

Labidi, J
Farquhar, J
Alexander, CM O'D
et al.

Publication Date

2017

DOI

10.1016/j.gca.2016.09.036

Peer reviewed

Mass independent sulfur isotope signatures in CMs: Implications for sulfur chemistry in the early solar system

Author links open overlay panel J.Labidi[a] J.Farquhar[b] C.M.O'D.Alexander[c] D.L.Eldridge[b] H.Oduro[d]
Show more

https://doi.org/10.1016/j.gca.2016.09.036 Get rights and content

Abstract

We have investigated the quadruple sulfur isotopic composition of inorganic sulfur-bearing phases from 13 carbonaceous chondrites of CM type. Our samples include 4 falls and 9 Antarctic finds. We extracted sulfur from sulfides, sulfates, and elemental sulfur (S^0) from all samples. On average, we recover a bulk sulfur (S) content of 2.11 ± 0.39 wt.% S (1σ). The recovered sulfate, S^0 and sulfidecontents represent 25 ± 12%, 10 ± 7% and 65 ± 15% of the bulk S, respectively (all 1σ). There is no evidence for differences in the bulk S content between falls and finds, and there is no correlation between the S speciation and the extent of aqueous alteration. We report ranges of $\Delta^{33}S$ and $\Delta^{36}S$ values in CMs that are significantly larger than previously observed. The largest variations are exhibited by S^0, with $\Delta^{33}S$ values ranging between −0.104 ± 0.012‰ and +0.256 ± 0.018‰ (2σ). The $\Delta^{36}S/^{33}S$ ratios of S^0 are on average −3.1 ± 1.0 (2σ). Two CMs show distinct $\Delta^{36}S/^{33}S$ ratios, of +1.3 ± 0.1 and +0.9 ± 0.1. We suggest that these mass independent S isotopic compositions record H_2S photodissociation in the nebula. The varying $\Delta^{36}S/\Delta^{33}S$ ratios are interpreted to reflect photodissociation that occurred at different UV wavelengths. The preservation of these isotopic features requires that the S-bearing phases were heterogeneously accreted to the CM parent body. Non-zero $\Delta^{33}S$ values are also preserved in sulfide and sulfate, and are positively correlated with S^0 values. This indicates a genetic relationship between the S-bearing phases: We argue that sulfates were produced by the direct oxidation of S^0 (not sulfide) in the parent body. We describe two types of models that, although imperfect, can explain the major features of the CM S isotope compositions, and can be tested in future studies. Sulfide and S^0 could both be condensates from the nebula, as the residue and product, respectively, of incomplete H_2S photodissociation by UV light (wavelength <150 nm). This idea requires that FeS formation and the S^0 condensation co-occur. As an alternative, ice accretion to the CM parent body could allow the delivery of S-MIF in CMs. In that case, sulfides would have been the only S-bearing condensate in CM precursors, and S^0 would have been derived from the oxidation of H_2S trapped in ices, after its photodissociation at low temperature (<500 K) in the nebula. In our models, the observations of H_2S UV photodissociation is required to

occur at the disk surface, and allowed in nebular environments with canonical C/O ratios. Vertical motions in the disk would redistribute phases that condensed at high altitude to the midplane, where they accreted in the phases that make up the chondritic matrix.

- **Previous** article
- **Next** article

Keywords

Sulfur isotope
Photodissociation
Early solar system
Chondrites

1. Introduction

The sulfur (S) isotopic compositions of meteorites reflect a complex collection of nucleosynthetic, physical, and chemical processes that occurred both in nebular and asteroidal environments. The magnitude of mass-independent S isotope signatures in meteorites is typically sub-permil, nowhere near as large as those seen for oxygen. However, a growing body of evidence suggests that they are widespread, and these signatures have largely been interpreted to reflect photochemical reactions (Cooper et al., 1997, Farquhar et al., 2000a, Rai et al., 2005, Chakraborty et al., 2013, Antonelli et al., 2014).

Subtle but widespread $\Delta^{33}S$ variations have been reported in achondrites and iron meteorites, with $\Delta^{33}S$ variations extending up to 0.050‰ for bulk S (Farquhar et al., 2000a, Rai et al., 2005, Antonelli et al., 2014, Defouilloy et al., 2016). Aubrites carry only small ^{33}S enrichments relative to Canyon Diablo Troilite (CDT) for their bulk S, with a mean $\Delta^{33}S$ value of +0.015 ± 0.006‰ (n = 6, Rai et al., 2005, 2σ), but an oldhamite (CaS) mineral separate from the Norton County aubrite was reported to have a $\Delta^{33}S$ value of +0.161 ± 0.012‰ (2σ, Rai et al., 2005). DeFouilloy et al. (2016) reported near zero to significantly negative $\Delta^{33}S$ values in oldhamites (CaS) from aubrites, down to −0.085 ± 0.020‰ (2σ) for Norton County. Because the Rai et al. (2005) result constitutes the highest $\Delta^{33}S$ value in the meteorite inorganic S record, oldhamite was suggested as a carrier for S-MIF in aubrites and other meteorites (Rai et al., 2005). Oldhamite being a relatively refractory mineral would have acquired its S-MIF signatures in the inner, hotter and reducing parts of the nebula (Rai et al., 2005). After condensation, a heterogeneous distribution of CaS grains in the precursors of

achondrites could account for their variable $\Delta^{33}S$ values (Rai et al., 2005). Antonelli et al. (2014) also suggested that refractory sulfides, such as oldhamite, would have acted as carriers of S-MIF to iron meteorite precursors.

In contrast to the achondrites, the chondrites have been considered to preserve evidence for predominantly mass dependent sulfur. Gao and Thiemens (1993) reported mass dependent S isotope ratios in seven carbonaceous chondrites, three of which were CM chondrites (Mighei, Allan Hills (ALH) 84029, and Murchison), and observations of S-MIF signature have been considered to be isolated occurrences. One of these observations includes S-MIF identified in a minor component of the CV chondrite Allende (Rees and Thode, 1977: $\Delta^{33}S = +1.1 \pm 0.1‰$ 2σ). A second observation is for the sulfonic organic acids from the Murchison CM chondrite that carry $\Delta^{33}S$ values between −0.40 ± 0.05‰ and +2.00 ± 0.05‰ (Cooper et al., 1997, 2σ). Smaller magnitude S-MIFs were also observed in chondrules of the Djahala ordinary chondrite(Rai and Thiemens, 2007: $\Delta^{33}S = +0.10 \pm 0.03‰$, 2σ). Rees and Thode (1977) considered their observation as a possible nucleosynthetic anomaly, whereas Cooper et al. (1997)suggested that the organic acids S isotopic compositions reflected the composition of photo-processed interstellar S. Rai and Thiemens (2007) envisioned a very different scenario that tied anomalies in chondrules to those in achondrites. The X-wind astrophysical model (Shu et al., 1997) was suggested as a way to redistribute CaS grains from a region close to the Sun where they formed (and captured S-MIF) to other parts of the early solar nebula where the precursors to achondrites formed (Rai et al., 2005). This model was favoured to account for the $\Delta^{33}S$ value in sulfides extracted from Djahala (H3.8) chondrules (+0.10 ± 0.03‰, 2σ), because it provides a “mechanism for chondrule precursors to be irradiated with high energy UV light from the early Sun” (Rai and Thiemens, 2007).

The X-wind model is, however, hard to reconcile with several major features of chondrites. For example, it predicts highly oxidizing formation conditions for CAIs in the X-region, due to the removal of H_2 (Shu et al., 2001). However, oxygen barometers of CAI formation indicate a gas of solar composition (Simon et al., 2007). In addition, the X-wind model does not allow chondrules to form from material containing primary S, as the starting temperatures experienced by the precursors of chondrules would be too high (∼1100 K in Shu et al., 2001, which is ∼400 K above the FeS condensation temperature). Primary and secondary Fe sulfides are, however, common phases in chondrules (i.e., Tachibana and Huss, 2005, Marrocchi and Libourel, 2013). For more details, the reader is referred to review contributions (Krot et al., 2009, Desch et al., 2010).

Carbonaceous chondrites of CM type are often considered as among the most primitive chondrites (e.g., Huss et al., 2003), although they have clearly experienced varying degree of aqueous alteration (e.g., Rubin et al., 2007, Alexander et al., 2013, Howard et al., 2015 and references therein). The CMs have amongst the highest bulk S contents of any chondrite group (Burgess et al., 1991, Dreibus et al., 1995), and host various S-bearing phases, including Ni-Fe sulfides and tochilinite, elemental S (S^0), and sulfates (Gao and Thiemens, 1993, Airieau et al., 2005, Rubin et al., 2007, Bullock et al., 2010). These meteorites may thus have recorded and preserved the complex S chemistry that occurred in the nebula and during parent body processes. Here, we report S isotope data for 13 CM carbonaceous chondrites that preserve anomalous $\Delta^{33}S$ values. We show that a photolytic origin in the hotter, inner parts of the solar nebula, combined with a mixing process such as that provided by the X-wind does not explain the occurrence of S-MIF in CMs, and may not be required to account for S-MIF in achondrite parent bodies. Our data support the idea that S-MIF was produced by H_2S photolysis under low temperature conditions near the surface of the disk, and imply that S-MIF can potentially be produced at various heliocentric distances. We discuss whether it could constitute a viable alternative to the idea of a refractory high-temperature sulfide condensate such as oldhamite as the origin of the signature in the parent bodies of achondrites and iron meteorites as well as in chondrules.

2. Samples

Thirteen meteorites were studied here, including four observed falls and nine Antarctic finds (Table 1). Samples were chips from the interiors of the meteorites taken well away from the fusion crust to minimize the effects of terrestrial contamination and modification during atmospheric entry. Other than the Antarctic samples allocated by the Johnson Space Center that were stored under N_2 atmosphere for curation and subsequently in desiccators, no special precautions were taken with regard to sample storage history. The samples were selected to cover the full range of CM aqueous alteration (Table 1). These CMs were previously divided into unheated and heated meteorites based on their water contents and hydrogen isotopic composition (Alexander et al., 2013). Here, 12 unheated CMs and one heated CM were investigated.

Table 1. A list of the studied samples, with estimated bulk H contents in water/OH and bulk δD composition, as reported in Alexander et al. (2013). Sample identification is given for falls. BM stands for British Museum, ASU for Arizona State University, and USNM for the Smithsonian institute. All the samples are of CM2 type except PCA 91084, which is a heated CM (Alexander et al., 2007, Alexander et al., 2013). Two petrologic classification scales are presented here, after Alexander et al. (2013). On the

first scale, the samples are distributed according to their petrologic types using a scale from 2 to 3, based on correlations between bulk H isotopic compositions and the petrologic criteria of Browning et al. (1996) and Rubin et al. (2007). On the other scale, the samples are on a scale of 1–3 based on bulk water/OH H contents.

	Fall/find	Sample ID	Petrologic types		H content and isotope composition in bulk sample	
			Based on H content[a]	Based on δD[b]	Water/OH H (wt%)[c]	δD (‰)[d]
Banten	Fall	USNM 6017	1.7	2.5	0.91	−32.4
Cold Bokkeveld	Fall	BM. 1727	1.3	2.2	1.22	−168.3
Murchison	Fall	BM.1988,M23	1.6	2.4	0.96	−61.7
Nogoya	Fall	ASU #556.2	1.1	2.1	1.31	−181.5
ALH 84029	Find	n.a.	1.2	2.1	1.30	−184.1
DOM 08003	Find	n.a.	1.1	2.2	1.36	−137.0
DOM 08013	Find	n.a.	1.8	2.7	0.85	47.2
GRA 98074	Find	n.a.	1.6	2.6	1.00	−14.1
LEW 85312	Find	n.a.	1.8	2.9	0.83	126.3
LEW 87022	Find	n.a.	1.4	2.3	1.09	−112.9
MCY 05230	Find	n.a.	1.8	2.5	0.87	−17.6
PCA 91084[e]	Find	n.a.	1.8	2.4	0.85	−74.6
TIL 91722	Find	n.a.	1.9	2.7	0.79	53.7

a

Petrologic type on a scale from 1 to 2, see Alexander et al. (2013); Petrologic type = $3 - H_{water/OH}/0.7$.

b

Petrologic type on a scale from 2 to 3, see Alexander et al. (2013); Petrologic type = (δD + 994)/383.

c

Typical 1σ uncertainty is <0.03 wt%.

d

Typical 1σ uncertainty is <10 ‰.

e

Heated CM.

Samples of meteorite falls include Murchison and Cold Bokkeveld (allocated by the British Natural History Museum), as well as Banten and Nogoya (allocated by the Smithsonian Institution). With the exception of Murchison and Cold Bokkeveld, all the processed powders were previously investigated for their bulk hydrogen, nitrogen and carbon isotope compositions (Alexander et al., 2012, Alexander et al., 2013). The H, N and C isotope compositions of their insoluble organic matter (IOM) (Alexander et al., 2007, Alexander et al., 2010), as well as their carbonate C and O isotope composition (Alexander et al., 2015) have also been reported for most of the samples. The H contents and isotope compositions (Alexander et al., 2013) and bulk mineralogies (Howard et al., 2015) of the samples have been used to place the samples on an alteration sequence. Murchison and Cold Bokkeveld were also investigated by Alexander et al., 2007, Alexander et al., 2012, Alexander et al., 2013, Alexander et al., 2015, but on different samples.

The samples were crushed in a steel percussion mortar and then ground in an agate mortar to pass through 100–150 μm sieves. About 200 mg aliquots were taken from the ~1000 mg powdered samples that had been previously studied by Alexander et al., 2012, Alexander et al., 2013, Alexander et al., 2015.

3. Methods

3.1. Extraction

Various authors have reported the occurrence of S^0 in CIs and CMs, in addition to ubiquitous sulfides. Monster et al. (1965), Kaplan and Hulston (1966) and Gao and Thiemens (1993)used wet chemistry techniques to recover S^0. The main strategy these studies employed was to process the samples in organic solvents to selectively dissolve S^0. Burgess et al. (1991) used a stepped combustion technique to survey the relative and absolute abundances of S^0 in various carbonaceous chondrites (CI, CM and CR). Sulfates have also been previously observed in carbonaceous chondrites, especially in CMs. Fuchs et al. (1973) observed gypsumplates in both Murchison and Cold Bokkeveld. Although petrographic studies of CMs report sulfides to be the

dominant (if not the exclusive) observed S-bearing phase (e.g., Bullock et al., 2005, Bullock et al., 2010), Gao and Thiemens (1993)report sulfate as being the dominant S-bearing pool in CMs. Hence, we developed an extraction protocol in anticipation of the complex S speciation in CMs. We present here a technique for redox-specific S extraction out of CMs that allows for determination of the S speciation, abundances and isotopic compositions for three recovered S-pools: S^0, sulfate, and sulfide.

We used sequential extraction techniques to extract S from these three pools. Organic S was not the target of this study, and will not be further discussed. The protocol is summarized in Fig. 1 and is described below. Samples were first processed in N_2-flushed Milli-Q water for 24 h at room temperature to dissolve sulfate and soluble organic compounds. After centrifugation and extraction of the water, we added $BaCl_2$ to the water solutions leading to the precipitation of $BaSO_4$ from dissolved sulfate. This step yielded the equivalent of from 1100 ± 100 ppm S (MacKay Glacier (MCY) 05230) to 12,900 ± 100 ppm S (Pecora Escarpment (PCA) 91084). For 10 of the 13 samples, the sulfate contents were more tightly constrained to 4500–6000 ppm S. After rinsing with Milli-Q water, this extraction was repeated and yielded non-detectable (<50 ppm) sulfate in the repeat, indicating that the first extraction was quantitative. It also indicates that our protocol does not lead to sulfate formation via sulfide oxidation, as it would otherwise yield significant SO_4^{2-} amounts in the repeat as well. The S in our $BaSO_4$ precipitates was then reduced to H_2S and recovered as silver sulfide (Ag_2S) using the standard technique described by Thode et al. (1961).

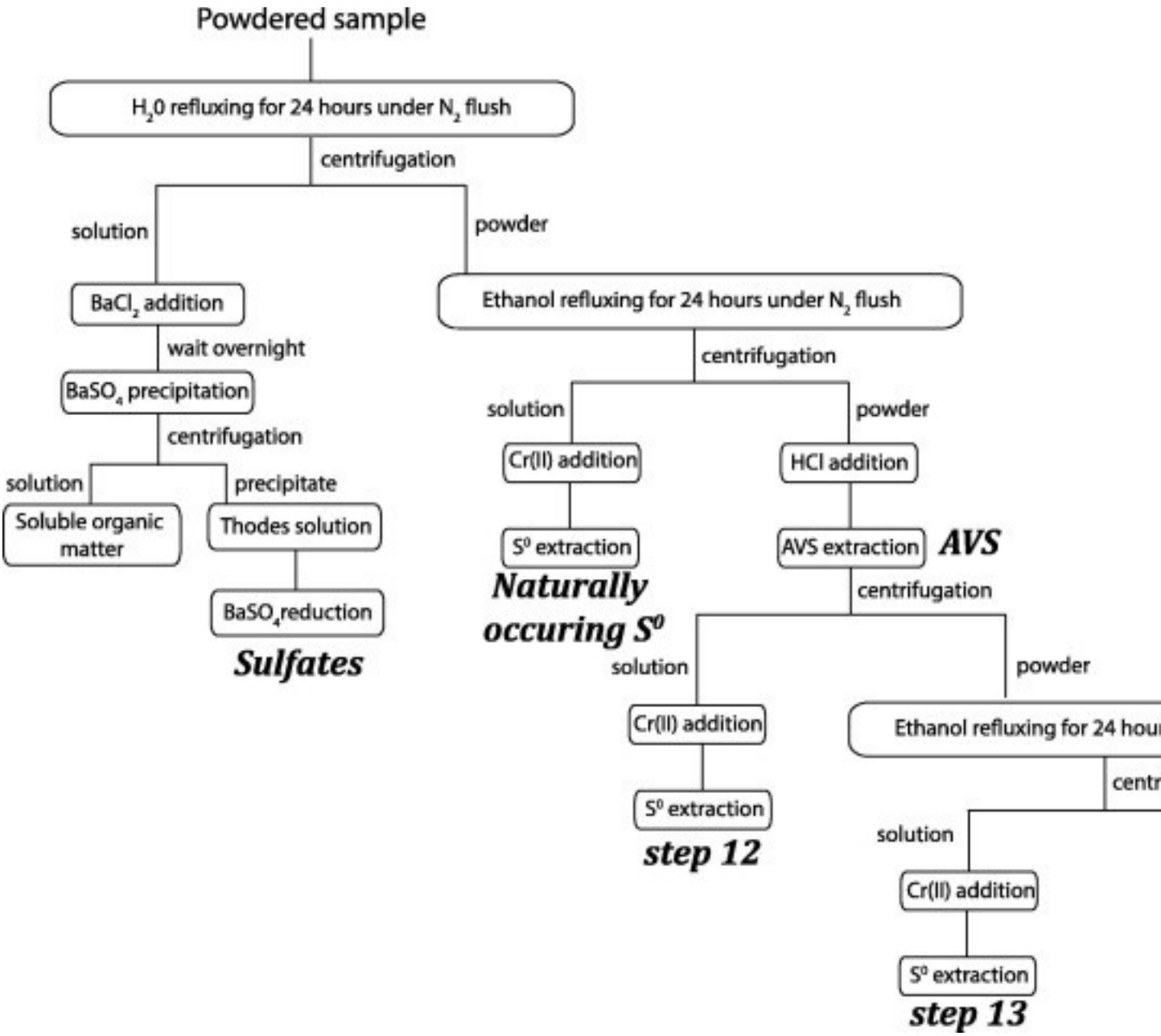

1. Download high-res image (366KB)
2. Download full-size image

Fig. 1. Analytical flow diagram for sulfate, S^0, and sulfide extraction from CMs. Soluble and insoluble organic compounds were also isolated, but are not studied here. Sulfides compositions are estimated by pooling the AVS, step 12, and step 13 extracts (see Sections 3.1 Extraction, 5.1.3 Sulfide and Appendix A).

Elemental sulfur is insoluble in water at room temperature (19 ± 6 nM; Boulegue, 1978). After rinsing, the rock samples were processed in N_2-flushed ethanol (reagent grade, anhydrous 200 proof) for 72 h at room temperature to extract S^0. The ethanol solutions

then underwent reaction with a sub-boiling (~80 °C) 5 N HCl solution for 1 h. At this step, any hypothetical ethanol-soluble, acid-volatile sulfide phases would be converted into H_2S and recovered as Ag_2S. This step, however, only yielded blank level amounts of S for all samples (<1 ppm S), ruling out the occurrence of any such phases. The solutions were then processed in sub-boiling $CrCl_2$ + HCl solutions for 3 h using the standard technique described by Canfield et al. (1986), which quantitatively reduces S^0 to H_2S via the oxidation of Cr^{2+} to Cr^{3+} and allows for the recovery of H_2S as Ag_2S. Between 400 ± 100 ppm and 5500 ± 100 ppm S was extracted during this step, with most samples yielding <2500 ppm S. Aliquots of these ethanol extracts were also processed for independent S^0 analysis via High Performance Liquid Chromatography (HPLC) with UV-detection (Kamyshny et al., 2009). An Agilent 1200 HPLC system with an Agilent Eclipse XDB-C18 column (4.6 × 150 mm; 5 µm particle size) was utilized with an isocratic 100% HPLC-grade methanol mobile phase. Calibrations for the quantification of S^0 were prepared from stock solutions of S^0 (reagent grade refined S powder, 100 mesh; Sigma Aldrich) dissolved in ethanol (reagent grade, anhydrous 200 proof) over a concentration range of 1–1000 µM (retention times of ca. 5.5 min with our method). The HPLC determinations of S^0 matched our wet chemistry extractions across the large range of observed S abundances within ±10% (Supplementary Fig. 1 and Table 2). The convergence of these two independent approaches strongly indicates that the S extracted with ethanol is predominately in the form of S^0. We further argue below that this S-bearing pool is naturally occurring S^0 in the CMs. As for the water extractions, this step was repeated and did not yield any significant additional S extraction (i.e., always <2% of what was extracted in the first step), indicating that the first extraction was quantitative. It also indicates that the protocol did not lead to the formation of S^0 from sulfide oxidation, as it would otherwise lead to significant S^0 amounts in the repeat.

Table 2. The sulfur contents and speciation in the 13 studied CMs, obtained with our wet chemistry technique. Unless stated otherwise, the S contents were obtained by weighing of Ag_2S generated after chemical extraction of the S from the meteorites. The uncertainty in the abundances is ~100 ppm (1σ) and S content estimates for individual meteorites were rounded to the nearest 100. For S^0, the abundance values obtained via High Performance Liquid Chromatography (HPLC) are also presented. The AVS, step 12 and step 13 pools refer to the fractions of extracted sulfide S using our extraction protocol. The AVS pool (for Acid Volatile Sulfur) is the H_2S generated when the CM powders were processed in hot HCl. Step 12 and 13 reflect the collection of S^0 that had been produced during the AVS step (reaction 1, see Section 3.1). These three extracts were pooled by mass balance and considered to represent the bulk sulfide. See Sections 3.1 Extraction, 5.1.3 Sulfide, and Appendix Afor details.

	Mass processed (mg)	Sulfate	S^0	Step 13	Step 12	AVS	Sulfide	Sum	S^0HPLC
ALH 84029	206	4800	5500	8500	500	500	9500	19,800	5800
Banten	197	6500	800	11,000	900	700	12,600	19,900	900
Cold Bokkeveld	214–436[a]	5300	1300	12,000	500	200	12,700	19,300	1100
DOM 08003	194	6800	2800	8600	200	1000	9800	19,400	3700
DOM 08013	192	6300	3100	17,600	1000	2200	20,800	30,200	3200
GRA 98074	198	2400	1000	13,100	500	100	13,700	17,100	700
LEW 85312	198	6000	400	12,700	700	1300	14,700	21,100	500
LEW 87022	206	2000	1200	14,100	700	3100	17,900	21,100	1200
MCY 05230	202	1100	1300	12,300	200	3100	15,600	18,000	1300
Murchison	201–202[a]	5900	1600	7500	600	200	8300	15,800	12,300
Nogoya	204	3700	1400	16,100	800	900	17,800	22,900	1400
PCA 91084	211	13,000	3200	10,800	500	100	11,400	27,600	2100
TIL 91722	208	5955	1500	11,000	500	1900	13,400	20,855	1300
Average		5400	1900	11,900	600	1200	13,700	21,000	2700
Std dev		3000	1400	2900	300	1100	3600	4000	3200

All abundances are given in ppm S.

a Range of values for replicates. See Table 4. S abundance estimates are averages of the replicates.

After rinsing with Milli-Q water, the rock samples were digested in a sub-boiling 5 N HCl solution for 3 h. H_2S was evolved from all samples (recovered as Ag_2S) and is referred to as the acid-volatile S (AVS) fraction. Such fractions are usually considered to be the products of monosulfide digestion (e.g., FeS, NiS, but not pyrite, see Canfield et al.,

1986). Between 100 and 3100 ppm S were extracted at this step. For three samples, AVS extractions yielded ~100 ppm, which was insufficient to analyze their isotopic compositions.

Solid residues and acid solutions from the HCl treatments were then transferred to Falcon™ tubes for centrifugation. The acid solution was subsequently transferred back to the distillation apparatus, and underwent reaction with a sub-boiling $CrCl_2$ solution (after Canfield et al., 1986). H_2S was evolved for all samples and recovered as Ag_2S. This fraction is referred to as step 12. Between 200 ppm S and 1000 ppm S were extracted at this step. The solid residue of the AVS extraction was processed in N_2-flushed ethanol (reagent grade, anhydrous 200 proof) for 72 h at room temperature. The ethanol extracts were then processed in a sub-boiling 5 N HCl solution for 1 h. As for the first ethanol extraction steps (step 2), this never yielded detectable AVS, ruling out the occurrence of any acid volatile sulfide phases in the ethanol solutions. The solutions were then processed in sub-boiling $CrCl_2$ solution for 3 h. Again, evolved H_2S was recovered as Ag_2S. Between 5400 ppm and 19,000 ppm S was extracted, which represent roughly an order of magnitude more than in step 12. This fraction is referred to as step 13. The AVS, step 12 and step 13 extracts were analyzed separately for their S isotopic compositions, and the results are given in Table 2. These three extractions (AVS, step 12 and step 13) were pooled by mass balance and considered to represent the bulk sulfide (see below).

3.2. Isotopic analysis

Weighed silver sulfide samples were wrapped in Al-foil and placed in Ni-reaction vessels for fluorination with at least 10 times excess of pure F_2 at 250 °C overnight. The produced SF_6 was isolated from impurities with cryogenic and chromatographic techniques, as described in Bains-Sahota and Thiemens, 1988, Rumble et al., 1993 and modified by Ono et al. (2006). The volume of purified SF_6 was then measured with a manometer, and transferred to the dual inlet of a ThermoFinnigan MAT 253 isotope ratio gas-source mass spectrometer that was used to measure ion beams at m/z = 127+, 128+, 129+ and 131+. Once $\delta^n S$ are determined (n = 33, 34, 36), $\Delta^{33}S$ and $\Delta^{36}S$ are calculated ($\Delta^{33}S = \delta^{33}S - 1000((\delta^{34}S/1000 + 1)^{0.515} - 1)$ and $\Delta^{36}S = \delta^{36}S - 1000((\delta^{34}S/1000 + 1)^{1.90} - 1)$)). The results are given in Table 3. IAEA S1 values are used to evaluate our long-term accuracy and precision on standards, and to anchor our $\delta^{34}S$ to the V-CDT scale. Analyses of the S1 standard performed along with the CM analyses yield average $\delta^{34}S$, $\Delta^{33}S$ and $\Delta^{36}S$ values of −5.28 ± 0.09‰, +0.083 ± 0.008‰ and −0.78 ± 0.26‰ (n = 13, all 2 s.d.) relative to our reference gas.

Relative to the same reference gas, our CDT yield $\delta^{34}S$, $\Delta^{33}S$ and $\Delta^{36}S$ values at −4.88 ± 0.15‰, −0.035 ± 0.008‰ and −0.08 ± 0.08‰ (*n* = 6, all 2 s.d.). The S isotope shift for $\delta^{34}S$, $\Delta^{33}S$ and $\Delta^{36}S$ between CDT and S1 is comparable to what was obtained elsewhere (Ono et al., 2006, Labidi et al., 2012).

Table 3. The sulfur isotopic composition of all S extracts in the 13 studied CMs. We report 2σ uncertainties of 0.10, 0.012 and 0.25‰ for $\delta^{34}S$, $\Delta^{33}S$ and $\Delta^{36}S$ values, respectively, for all measurements with a SF_6 amount >1 µmol. When SF_6 amount <1 µmol (*n* = 4), we report 2σ uncertainties of 0.10, 0.018 and 0.35‰ for $\delta^{34}S$, $\Delta^{33}S$ and $\Delta^{36}S$ values, respectively.

		ALH 84029	Banten	Cold Bokkeveld	DOM 08003	DOM 08013	GRA 98074	LEW 85312	LEW 87022	MCY 05230	Murchison	Nogoy
S^0	$\delta^{34}S$ (‰) V-CDT	2.42	4.28	2.88	3.25	3.23	4.06	3.69	5.29	3.17	3.71	3.16
	$\delta^{34}S$ (‰) CDT	2.32	4.18	2.78	3.15	3.13	3.96	3.60	5.19	3.07	3.61	3.06
	$\Delta^{33}S$ (‰)	0.018	−0.001	−0.001	−0.034 (±0.018)	−0.085	−0.055	−0.080 (±0.018)	−0.104	0.256	0.243	−0.002
	$\Delta^{36}S$ (‰)	0.00	0.04	0.09	0.12 (±0.35)	0.07	0.23	–	0.34	0.32	0.23	0.20
SO_4	$\delta^{34}S$ (‰) V-CDT	−1.65	−0.66	−0.70	−1.22	−1.68	−0.15	−4.44	0.19	−2.42	−0.64	−1.92
	$\delta^{34}S$ (‰) CDT	−1.75	−0.76	−0.80	−1.31	−1.78	−0.25	−4.54	0.09	−2.52	−0.74	−2.02
	$\Delta^{33}S$ (‰)	0.058	0.040	0.023	0.006	−0.036	−0.019	−0.023	−0.036	0.143 (±0.018)	0.263	0.034
	$\Delta^{36}S$ (‰)	−0.28	−0.23	−0.09	−0.21	−0.25	−0.03	−0.30	−0.14	0.26 (±0.35)	−0.11	−0.20
AVS	$\delta^{34}S$ (‰) V-CDT	0.84	0.73	–	0.55	−0.38	–	0.20	1.15	0.84	–	1.35
	$\delta^{34}S$ (‰) CDT	0.75	0.63	–	0.45	−0.48	–	0.11	1.05	0.74	–	1.25
	$\Delta^{33}S$ (‰)	0.027	0.007	–	0.016	0.006	–	0.010	−0.022	0.113	–	0.016
	$\Delta^{36}S$ (‰)	0.25	−0.03	–	0.12	−0.26	–	−0.07	0.18	0.28	–	0.25

		ALH 84029	Banten	Cold Bokkeveld	DOM 08003	DOM 08013	GRA 98074	LEW 85312	LEW 87022	MCY 05230	Murchison	Nogoy
Step 12	$\delta^{34}S$ (‰) V-CDT	2.18	0.25	–	4.64	−0.03	0.50	1.07	1.15	3.90	–	0.34
	$\delta^{34}S$ (‰) CDT	2.08	0.15	–	4.54	−0.13	0.40	0.98	1.05	3.80	–	0.24
	$\Delta^{33}S$ (‰)	0.046	−0.050	–	0.000 (±0.018)	−0.027	−0.023	0.015	−0.096	0.118	–	0.033
	$\Delta^{36}S$ (‰)	0.80	−0.06	–	0.42 (±0.35)	0.02	−0.20	0.20	0.07	1.16	–	0.23
Step 13	$\delta^{34}S$ (‰) V-CDT	0.16	−0.06	–	−0.72	−0.50	−0.35	0.20	0.09	0.21	–	0.02
	$\delta^{34}S$ (‰) CDT	0.06	−0.16	–	−0.82	−0.60	−0.44	0.10	−0.01	0.11	–	−0.08
	$\Delta^{33}S$ (‰)	0.047	−0.037	–	0.007	0.013	−0.014	−0.075	−0.049	0.106	–	0.006
	$\Delta^{36}S$ (‰)	0.12	0.07	–	0.21	−0.10	−0.04	−0.11	−0.11	0.19	–	0.14
Bulk sulfide[a]	$\delta^{34}S$ (‰) V-CDT	0.27	−0.04	−0.53	−0.60	−0.48	−0.31	0.25	0.15	0.28	0.24	0.03
	$\delta^{34}S$ (‰) CDT	0.17	−0.14	−0.63	−0.70	−0.58	−0.41	0.15	0.05	0.18	0.14	−0.07
	$\Delta^{33}S$ (‰)	0.047	−0.038	0.015	0.007	0.011	−0.014	−0.070	−0.051	0.106	0.156	0.007
	$\Delta^{36}S$ (‰)	0.16	0.06	0.05	0.22	−0.09	−0.04	−0.09	−0.10	0.20	−0.01	0.14
Bulk S[b]	$\delta^{34}S$ (‰) V-CDT	0.40	−0.06	−0.32	−0.09	−0.35	−0.04	−1.01	0.43	0.32	0.24	−0.10
	$\delta^{34}S$ (‰) CDT	0.30	−0.16	−0.42	−0.19	−0.45	−0.14	−1.11	0.33	0.23	0.14	−0.20
	$\Delta^{33}S$ (‰)	0.041	−0.011	0.016	−0.001	−0.009	−0.017	−0.058	−0.053	0.119	0.207	0.011

	ALH 84029	Banten	Cold Bokkeveld	DOM 08003	DOM 08013	GRA 98074	LEW 85312	LEW 87022	MCY 05230	Murchison	Nogoy
$\Delta^{36}S$ (‰)	0.01	−0.03	0.02	0.06	−0.10	−0.02	−0.27	−0.08	0.22	−0.02	0.09

Typical 2σ uncertainties are 0.10‰, 0.012‰, and 0.25‰ for $\delta^{34}S$, $\Delta^{33}S$ and $\Delta^{36}S$ respectively.

a

Estimated by mass balance of AVS, step 12 and 13. 2σ uncertainties <0.10‰, 0.018‰, and 0.42‰ for $\delta^{34}S$, ^{33}S and $\Delta^{36}S$ respectively. Typically 0.10‰, 0.012‰, and 0.25‰.

b

Estimated by mass balance of S^0, SO_4, AVS, step 12 and 13. 2σ uncertainties <0.35‰, 0.020‰, and 0.50‰ for $\delta^{34}S$, $\Delta^{33}S$ and $\Delta^{36}S$ respectively. Typically 0.30‰, 0.012‰, and 0.25‰.

We use the CDT scale to anchor our $\delta^{34}S$, $\Delta^{33}S$ and $\Delta^{36}S$ values. We additionally report our $\delta^{34}S$ values on the V-CDT scale to allow comparisons with other datasets also reported relative to V-CDT (e.g., terrestrial mantle-derived rocks, Labidi et al., 2013). We obtained 2σ uncertainties of 0.10, 0.012 and 0.25‰ for $\delta^{34}S$, $\Delta^{33}S$ and $\Delta^{36}S$ values, respectively, for all measurements with a SF_6 amount >1 μmol. When the SF_6amount was <1 μmol (n = 4), we obtained 2σ uncertainties of 0.10, 0.018 and 0.35‰ for $\delta^{34}S$, $\Delta^{33}S$ and $\Delta^{36}S$ values, respectively (Table 3). The whole procedure of S extraction and isotope analysis was repeated once on Murchison, and twice on Cold Bokkeveld, to address sample heterogeneity at the scale of the studied powders (Table 4).

Table 4. The sulfur isotopic composition of all S extracts in Murchison and Cold Bokkeveld replicates. We report 2σ uncertainties of 0.10, 0.012 and 0.25‰ for $\delta^{34}S$, $\Delta^{33}S$ and $\Delta^{36}S$ values, respectively, for all measurements. The $\delta^{34}S$ values are given versus V-CDT. The uncertainty in the abundances is ∼100 ppm (1σ) and S content estimates for individual meteoriteswere rounded to the nearest 100.

Powder mass (mg)		Murchison				Cold Bokkeveld				
		Split one	Split two	Average of replicates	1σ	Split one	Split two	Split three	Average of replicates	1σ
		201	202			214	436	284		
Sulfur chemistry	Sulfate (ppm S)	5600	6200	5900	400	5500	4900	5500	5300	300
	S^0(ppm S)	1100	2100	1600	700	900	1600	1300	1,300	400
	Step 13 (ppm S)	5400	9700	7500	3000	7800	18,400	9900	12,000	5600
	Step 12 (ppm S)	300	1000	–	–	600	700	100	–	–
	AVS (ppm S)	Pooled with	200	–	–	Pooled with	100	300	–	–

Powder mass (mg)		Murchison				Cold Bokkeveld				
		Split one	**Split two**	**Average of replicates**	**1σ**	**Split one**	**Split two**	**Split three**	**Average of replicates**	**1σ**
		201	**202**			**214**	**436**	**284**		
		step 12				step 12				
	Sulfide (ppm S)	5700	10,900	8300	3700	8400	19,200	10,400	12700	5700
	Sum (ppm S)	12,400	19,100	15800	4700	14,800	25,700	17,200	19,300	5700
S^0	$\delta^{34}S$ (‰)	4.72	2.69	3.71	1.44	4.31	2.14	2.21	2.88	1.23
	$\Delta^{33}S$ (‰)	0.236	0.249	0.243	0.009	−0.007	0.008	−0.003	−0.001	0.008
	$\Delta^{36}S$ (‰)	0.49	−0.04	0.23	0.38	0.69	0.09	–	0.39	0.42
SO_4	$\delta^{34}S$ (‰)	−0.45	−0.82	−0.64	0.26	−0.69	−0.55	−0.87	−0.70	0.16
	$\Delta^{33}S$ (‰)	0.261	0.264	0.263	0.002	0.025	0.029	0.014	0.023	0.008
	$\Delta^{36}S$ (‰)	0.17	−0.39	−0.11	0.40	−0.03	−0.14	−0.09	−0.09	0.06
AVS	$\delta^{34}S$ (‰)	Pooled with step 12	3.39			Pooled with step 12	Too small	1.00		
	$\Delta^{33}S$ (‰)		0.171					0.006		
	$\Delta^{36}S$ (‰)		–					0.37		
Step 12	$\delta^{34}S$ (‰)	−3.30	1.78	−0.76	3.59	−1.39	1.14	−2.12	−0.79	1.71
	$\Delta^{33}S$ (‰)	0.054	0.186	0.120	0.093	−0.020	0.012	0.027	0.006	0.024
	$\Delta^{36}S$ (‰)	0.83	0.00	0.42	0.58	0.45	0.13	0.30	0.29	0.16
Step 13	$\delta^{34}S$ (‰)	0.28	0.25	0.27	0.02	−2.21	0.07	0.48	−0.56	1.45
	$\Delta^{33}S$ (‰)	0.141	0.176	0.159	0.025	0.006	0.022	0.020	0.016	0.009
	$\Delta^{36}S$ (‰)	0.07	−0.14	−0.04	0.15	0.10	0.02	−0.02	0.03	0.06
Bulk	$\delta^{34}S$	0.08	0.40	0.24	0.22	−2.15	0.11	0.45	−0.53	1.41

Powder mass (mg)		Murchison				Cold Bokkeveld				
		Split one	Split two	Average of replicates	1σ	Split one	Split two	Split three	Average of replicates	1σ
		201	202			214	436	284		
sulfide[a]	(‰)									
	$\Delta^{33}S$ (‰)	0.136	0.177	0.157	0.029	0.004	0.022	0.020	0.015	0.010
	$\Delta^{36}S$ (‰)	0.11	−0.13	−0.01	0.17	0.13	0.02	−0.01	0.05	0.07
Bulk S[b]	$\delta^{34}S$ (‰)	0.23	0.25	0.24	0.01	−1.21	0.11	0.16	−0.31	0.78
	$\Delta^{33}S$ (‰)	0.201	0.213	0.207	0.008	0.011	0.022	0.016	0.016	0.006
	$\Delta^{36}S$ (‰)	0.17	−0.20	−0.02	0.26	0.11	0.00	−0.04	0.023	0.078

Estimated by mass balance of AVS, step 12 and 13. resulting 2σ uncertainties are lower than 0.10‰, 0.018‰, and 0.42‰ for $\delta^{34}S$, $\Delta^{33}S$ and $\Delta^{36}S$ respectively. Typically 0.10‰, 0.012‰, and 0.15‰.

Estimated by mass balance of S^0, SO_4, AVS, step 12 and 13. resulting 2σ uncertainties are lower than 0.15‰, 0.020‰, and 0.50‰ for $\delta^{34}S$, $\Delta^{33}S$ and $\Delta^{36}S$ respectively. Typically 0.10‰, 0.012‰, and 0.15‰.

4. Results

4.1. Bulk S content

The S abundances in the five extracted S reservoirs of each sample are reported in Table 1, and shown in Fig. 2. Bulk S contents range between 1.72 ± 0.2 wt.% S (Graves Nunataks(GRA) 98074) and 3.01 ± 0.2 wt.% S (Dominion Range (DOM) 08013), and averages at 2.11 ± 0.39 wt.% S (1σ). There is no evidence for differences in the bulk S content between falls and finds. We find Antarctic finds to have an average bulk S content of 2.18 ± 0.43 wt.% (*n* = 9, 1σ), whereas the finds have an average of 1.95 ± 0.29 wt.% (*n* = 4, 1σ).

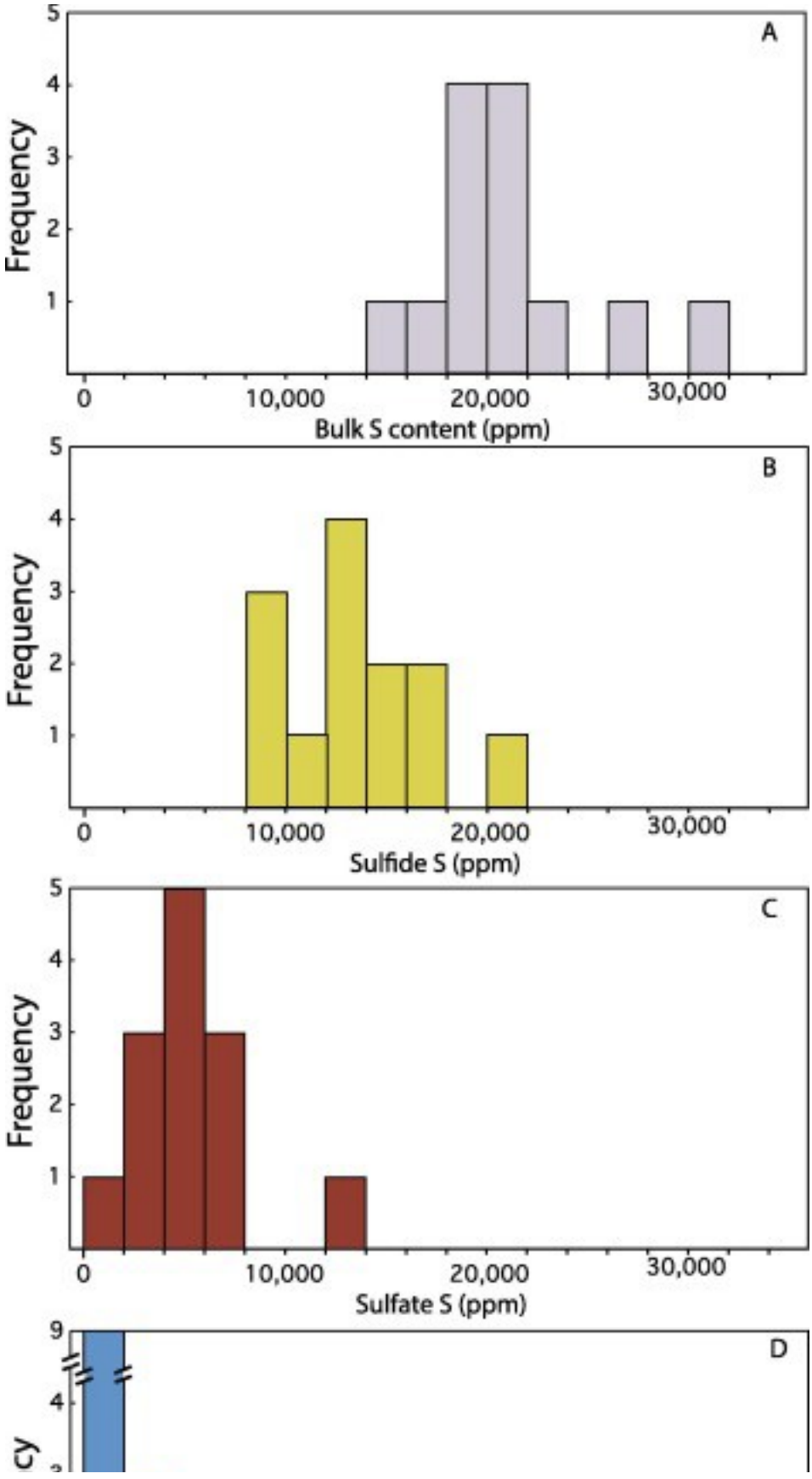
A
Frequency
5
4
3
2
1
0
10,000
20,000
30,000
Bulk S content (ppm)
B
Frequency
5
4
3
2
1
0
10,000
20,000
30,000
Sulfide S (ppm)
C
Frequency
5
4
3
2
1
0
10,000
20,000
30,000
Sulfate S (ppm)
D
9
4

1. Download high-res image (234KB)
2. Download full-size image

Fig. 2. Histograms of bulk S, sulfide, sulfate and S^0 contents of the 13 CMs studied here. For all samples except PCA 91084, sulfide is the dominant pool, whereas sulfate and S^0 are minor S-carrying reservoirs.

4.2. Sulfur speciation

For all the studied CMs, three S pools were systematically recovered and analyzed: Sulfide, sulfate, and S^0. The absolute abundances of each pool are given in Table 2 and shown in Fig. 2. The average sulfate content of our samples is 5400 ± 3000 ppm S (*n* = 13), but the contents range between 1100 ± 100 ppm S (MCY 05230) to 12,900 ± 100 ppm S (PCA 91084). Exclusion of these two extreme samples significantly decreases the standard deviation, leading to an average value of 5100 ± 1700 ppm S (*n* = 11, 1σ). Fall and find sulfate contents average at 5400 ± 1200 ppm S (*n* = 4, 1σ) and 5400 ± 3500 ppm S (*n* = 9, 1σ), respectively. The recovered sulfate contents represent 25 ± 12% of the bulk S of the studied CM chondrites (*n* = 13, 1σ, 6% for MCY 05230, 47% for PCA 91084).
Elemental S abundances recovered from the ethanolextractions average at 1900 ± 1400 ppm S, and range between 400 ± 100 ppm S (Lewis Cliffs (LEW) 85312) and 5500 ± 100 ppm S (Allan Hills (ALH) 84029). Fall and find S^0contents average at 1300 ± 300 ppm S (*n* = 4, 1σ and 2222 ± 1600 ppm S (*n* = 9, 1σ), respectively. These S^0contents represent 10 ± 7% of the bulk S (*n* = 13, 1σ, 2% for LEW 85312, 28% for ALH 84029).
Sulfides are the dominant pool in every chondrite studied here, with the exception of PCA 91084. Sulfide contents average at 13,700 ± 3600 ppm S, and ranges between 9500 ± 100 ppm S (ALH 84029) and 20,800 ± 100 ppm S (DOM 08013). These values represent 65 ± 15% of the bulk S (*n* = 13, 1σ, 48% for ALH 94029, 69% for DOM 08013). Note that PCA 91084 is the only CM where sulfide is not the dominant pool – sulfide and sulfate represent 41% and 47% of its bulk S, respectively. Fall and find sulfide contents average at 12,900 ± 3900 ppm S (*n* = 4, 1σ) and 14,100 ± 3700 ppm S (*n* = 9, 1σ), respectively.

4.3. Bulk S isotope compositions

The average bulk S $\delta^{34}S$ for all CMs is −0.08 ± 0.44‰ (1σ, *n* = 13) versus our CDT estimate. The average $\Delta^{33}S$ and $\Delta^{36}S$ are +0.021 ± 0.071‰ and 0.00 ± 0.09‰, respectively (1σ, *n* = 13), relative to CDT. The standard deviations for $\Delta^{33}S$ indicate a

much greater level of variability than reported by Gao and Thiemens (1993). Bulk S isotope compositions are plotted in Fig. 3: $\delta^{34}S$ values range from −1.11 ± 0.30‰ (LEW 85312) to +0.60 ± 0.30‰ (PCA 91084) relative to CDT (Fig. 3a). For $\Delta^{33}S$, bulk S values range from −0.058 ± 0.008‰ (LEW 85312) and +0.207 ± 0.008‰ (Murchison) relative to CDT (Fig. 3). Bulk S $\Delta^{36}S$ values range from −0.11 ± 0.25‰ (PCA 91084) and +0.22 ± 0.25‰ (MCY 05230) relative to CDT (Fig. 3b). Although the two CM with significantly positive $\Delta^{33}S$ both display positive $\delta^{34}S$, there is no systematic trend between $\delta^{34}S$ and $\Delta^{33}S$. $\Delta^{36}S$ values remain within uncertainties indistinguishable from CDT, and no trends appear in a $\Delta^{33}S$ σ $\Delta^{36}S$ plot. Additionally, no systematic S isotope difference was observed between falls and finds.

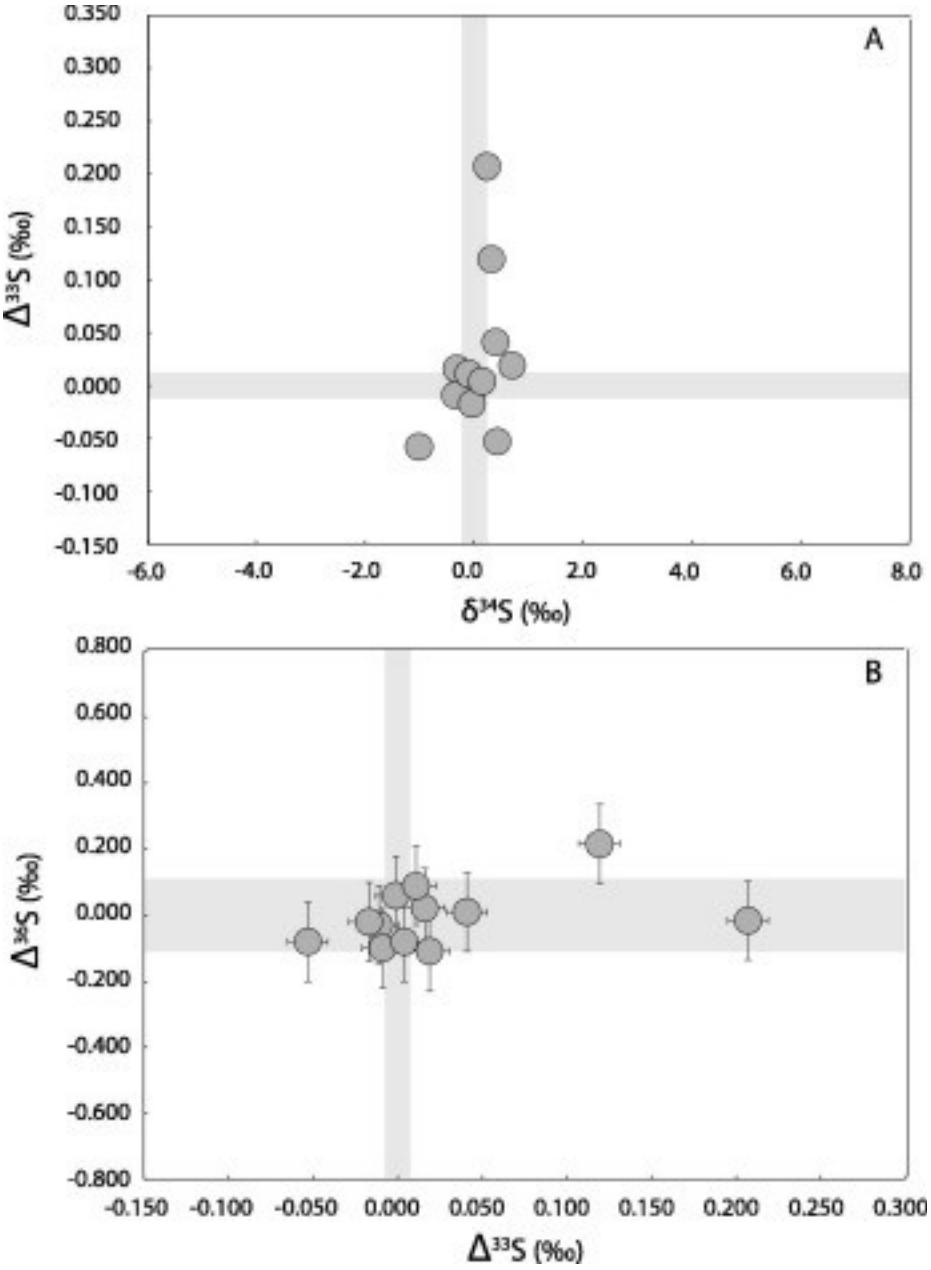

1. Download high-res image (164KB)
2. Download full-size image

Fig. 3. The quadruple S isotopic compositions of bulk S in the 13 CMs: (a) $\Delta^{33}S$ versus $\delta^{34}S$, and (b) $\Delta^{36}S$ versus $\delta^{34}S$. All the isotope data are given relative to CDT. The shaded areas are representations of CDT values and 2σ uncertainty. Whereas variability in $\delta^{34}S$ $\Delta^{36}S$ remains mostly within the reported uncertainties, resolvable variations are present in $\Delta^{33}S$, with values varying over a ~0.25‰ range. Over the 13 CMs, 5 samples have bulk S with non-CDT $\Delta^{33}S$ values.

4.4. S isotopic compositions of sulfide, sulfate and elemental sulfur

The S isotope compositions of the sulfide pools in the meteorites were estimated by combining the AVS, step 12 and step 13 results (Section 5.1.3). The calculated CM average sulfide $\delta^{34}S$ is −0.15 ± 0.33‰ (1σ, *n* = 13) relative to CDT, with values for individual meteorites ranging between −0.70 ± 0.15‰ (DOM 08003) and +0.18 ± 0.15‰ (MCY 05230). The average CM sulfide $\Delta^{33}S$ is + 0.015 ± 0.061‰ (1σ, *n* = 13), with values ranging between −0.070 ± 0.008‰ (LEW 85312) and +0.177 ± 0.008‰ (split 2, Murchison – Table 4). For $\Delta^{36}S$, average CM value is +0.04 ± 0.11‰ (1σ, *n* = 13), with values ranging between −0.10 ± 0.09‰ (LEW 87022) and +0.22 ± 0.23‰ (DOM 08003). The variability in the sulfide S isotopic compositions is comparable to the variability observed for bulk S, as illustrated by the comparable (or lower) standard deviations of the average values (Table 3).

Sulfate and S^0 have S isotope compositions that are more variable than those of the sulfide. The average CM $\delta^{34}S$ for sulfate is −1.15 ± 1.48‰ (1σ, *n* = 13) relative to CDT, with values ranging over ~6‰ between −4.54 ± 0.50‰ (LEW 85312) and +1.65 ± 0.50‰ (PCA 91084). There is no systematic trend between sulfate $\delta^{34}S$ and abundance (Table 2, Table 3), although PCA 91084 has both the highest $\delta^{34}S$ and the highest sulfate content (1.75 ± 0.50‰ and 12,900 ± 100 ppm S, respectively). PCA 91084 is the only heated CM in our suite (Alexander et al., 2012, Alexander et al., 2013). If PCA 91084 is excluded, the CM sulfate $\delta^{34}S$ average becomes −1.39 ± 1.28‰ (1σ, *n* = 12), which is the lowest across the S pools in CMs. The CM average $\Delta^{33}S$ for sulfate is +0.036 ± 0.084‰ (1σ, *n* = 13), with values ranging between −0.036 ± 0.008‰ (LEW 87022) and +0.263 ± 0.008‰ (Murchison). For $\Delta^{36}S$, the CM sulfate average is −0.16 ± 0.15 (1σ, *n* = 13), with values ranging between −0.33 ± 0.25‰ (TIL 91722) and +0.26 ± 0.25‰ (MCY 05230). Whereas the sulfate component of PCA 91084 has an extreme $\delta^{34}S$ compared other CMs, its $\Delta^{33}S$ and $\Delta^{36}S$ values are +0.016 ± 0.008‰ and −0.15 ± 0.25‰ respectively, i.e., within the range of the other CMs.

The average $\delta^{34}S$ for S^0 is +3.06 ± 1.63‰ (1σ, *n* = 13) relative to CDT, with values ranging between −1.84 ± 0.15‰ (PCA 91084) and +5.19 ± 0.15‰ (LEW 87022), representing a ~7‰ range. When all CMs are considered, no trend appears between the S^0 $\delta^{34}S$ values and contents. If PCA 91084 (the only heated CM) is excluded, the average becomes +3.46 ± 0.74‰ (1σ, *n* = 12), with the minimum value displayed by ALH 84029 at +2.32 ± 0.15‰ (~3‰ total range only). Elemental S is the S-bearing phase with the highest average $\delta^{34}S$. The average $\Delta^{33}S$ is +0.016 ± 0.113‰, with values ranging between −0.104 ± 0.008‰ (LEW 87022) and +0.256 ± 0.008‰ (MCY 05230). While the S^0 pool is the least abundant S-bearing phase in our CMs, it is the pool with the highest $\Delta^{33}S$ variability. The $\Delta^{36}S$ average is +0.159 ± 0.172‰ (1σ, *n* = 13), with

values ranging from −0.23 ± 0.25‰ (PCA 91084) to +0.39 ± 0.42‰ (Cold Bokkeveld, see Table 4). As for sulfate, S^0 in PCA 91084 has an extreme $\delta^{34}S$ compared other CMs, but its $\Delta^{33}S$ and $\Delta^{36}S$ values, of +0.045 ± 0.008‰ and −0.23 ± 0.25‰, respectively, are, within uncertainties in the range of the other CMs.

In comparison with Murchison and MCY 05230, all our meteorites lie relatively close to the origin in a $\Delta^{33}S$ vs. $\Delta^{36}S$ plot. In detail, they display $\Delta^{33}S$ values ranging between indistinguishable from CDT to significantly negative (Fig. 4, Fig. 5). The data form a rough array with a slope of −3.9 ± 2.2 in the $\Delta^{33}S$ vs. $\Delta^{36}S$ plot (2σ, Fig. 5). Only Murchison and MCY 05230 are clearly outside of this main trend. This is also observed for their bulk S (Fig. 3b), and is a result of their sulfide, sulfate and S^0 extracts all showing large positive $\Delta^{33}S$ associated with near-zero $\Delta^{36}S$ (Fig. 5). Again, no systematic S isotope differences were observed between falls and finds.

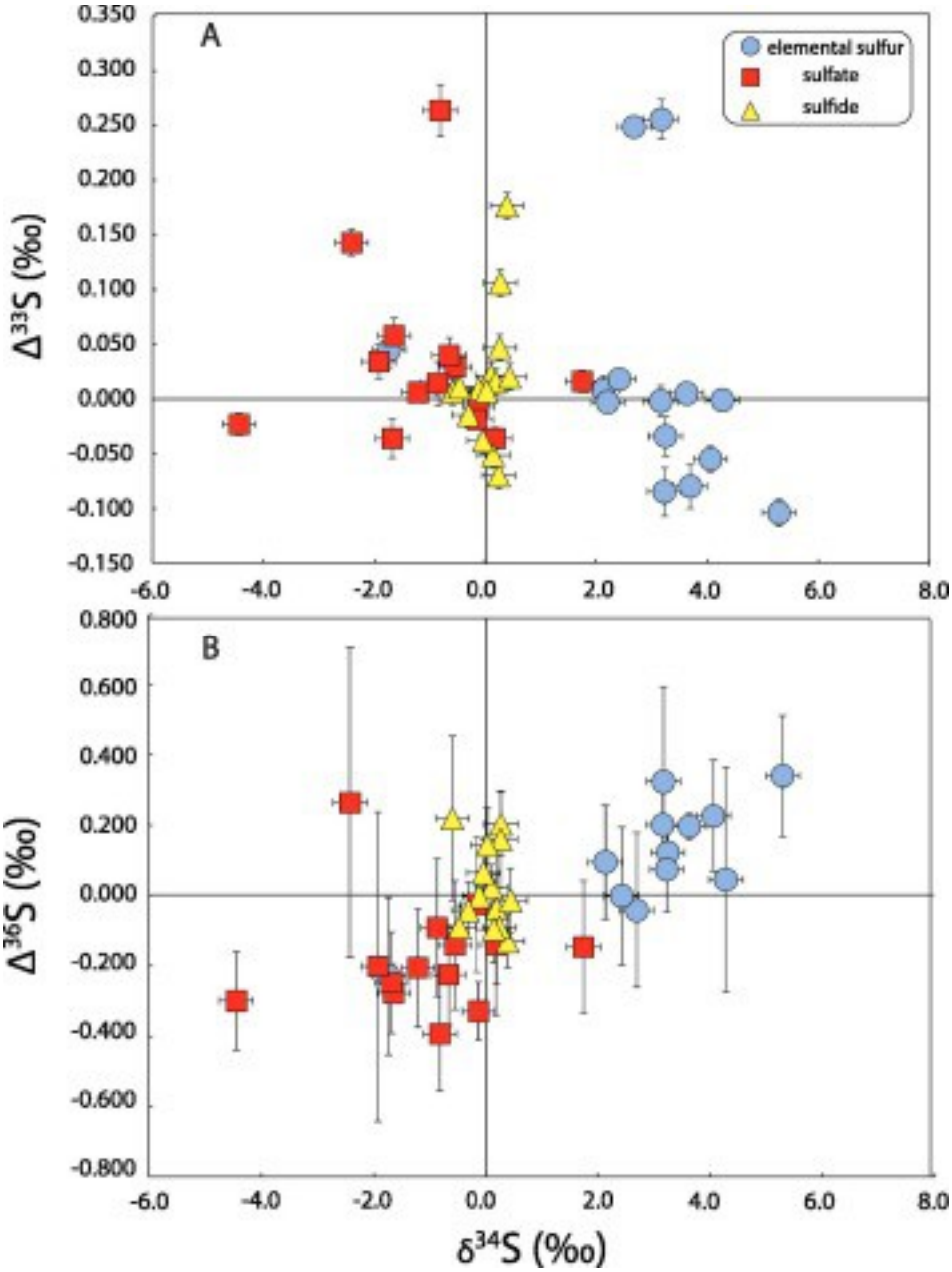

1. Download high-res image (235KB)
2. Download full-size image

Fig. 4. For the 13 CMs, the quadruple S isotopic compositions of sulfide (yellow triangles), sulfate (red squares) and S^0 (blue circles) in the 13 CMs: (a) $\Delta^{33}S$ versus $\delta^{34}S$, and (b) $\Delta^{36}S$ versus $\delta^{34}S$. All the isotope data are given relative to CDT. Large $\Delta^{33}S$ variations are recorded in the S^0 extracts. The $\Delta^{33}S$ values vary over a ~0.35‰ range. This is also observed in the sulfate extracts, but the sulfide extracts mimic the bulk S compositions with moderate $\Delta^{33}S$ variations that range over ~0.2‰. In contrast to bulk S, resolvable $\delta^{34}S$ $\Delta^{36}S$ are present in the individual S components. A ~10‰ $\delta^{34}S$ range is observed between sulfate and S^0. The $\Delta^{36}S$ values vary over a ~1‰ range. (For

interpretation of the references to colour in this figure legend, the reader is referred to the web version of this article.)

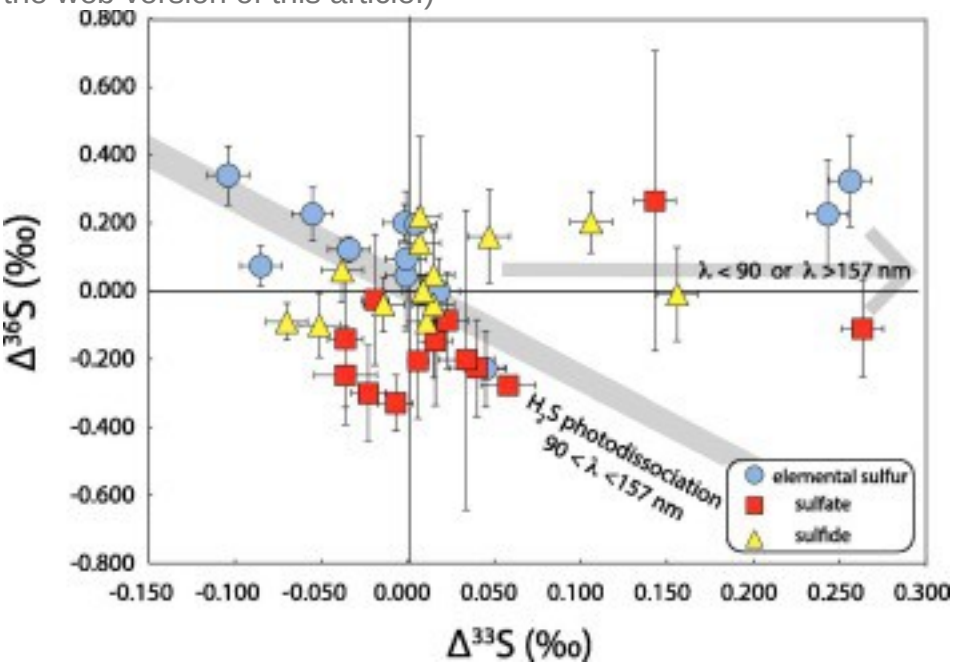

1. Download high-res image (162KB)
2. Download full-size image

Fig. 5. $\Delta^{33}S$ versus the $\Delta^{36}S$ values of individual S-carrying pools in the 13 CMs. All the isotope data are given relative to CDT. The samples show a rough negative trend, with a slope of −3.9 ± 2.2 (2σ). The slope is better defined if only S^0 is considered, with a value of −3.1 ± 1.0 (2σ). Murchison and MCY 05230 are excluded from this main trend, both showing positive $\Delta^{36}S/\Delta^{33}S$ values for their sulfide, sulfate and S^0. The main trend and the deviations from the main trend (for Murchison and MCY 05230) provide information on the type of H_2S photodissociation that occurred in the nebula(see Section 5.4).

4.5. Duplicates

The samples of Murchison and Cold Bokkeveld were of sufficient size to allow us to perform replicates of our whole S extraction protocol (Table 4). Two and three replicates were produced for Murchison and Cold Bokkeveld, respectively. Whereas the sulfate extractions yielded S contents that were consistent within 10% between replicates (and indistinguishable isotope compositions), the S^0 and sulfide extractions showed variations of up to roughly a factor of two. The $\delta^{34}S$ values of the sulfide duplicates for Murchison remain close, −0.02 ± 0.30‰ (5700 ppm S) and +0.30 ± 0.30‰ (10,800 ppm S), despite the factor of two difference in sulfide S contents. In contrast, $\Delta^{33}S$ variations for sulfide S are outside of four times the estimated analytical uncertainty, with values of +0.136 ± 0.010‰ (5700 ppm S), and +0.177 ± 0.010‰ (10,800 ppm S). The $\delta^{34}S$ values

of S^0 are resolvable across the two Murchison duplicates, being + 4.62 ± 0.15‰ (1100 ppm S) and +2.59 ± 0.15‰ (2100 ppm S). In contrast, their $\Delta^{33}S$ values are indistinguishable from one another, being +0.236 ± 0.008‰ (1100 ppm S) and +0.247 ± 0.008‰ (2100 ppm S). These variations are significant but remain lower than the overall variations between Murchison and other CMs. In contrast with Murchison, no $\Delta^{33}S$ variability was resolved between Cold Bokkeveld duplicates (Table 4).

5. Discussion

5.1. Evaluation of our S-extraction protocol

5.1.1. Sulfate

Gao and Thiemens (1993) report the sulfate contents of two pieces of Murchison (Field Museum, Chicago), one piece of ALH 84029, and one piece of Mighei. They extracted 6900 ppm S as sulfate from Mighei, which is similar to the range of sulfate concentrations observed in our CM extractions. The extractions by Gao and Thiemens (1993) of sulfate from two pieces of Murchison yielded 5600 and 6000 ppm S, which are indistinguishable from our extractions for this meteorite (Table 2). Their extraction of sulfate from ALH 84029 yielded 8000 ppm S, which is nearly twice the amount that we extracted (4800 ppm). Burgess et al. (1991)used combustion techniques to determine sulfate contents in Murchison, Mighei, Nogoya and Murray. They report 14,100 ppm S as sulfate for Murchison, and 14,500 ppm S as sulfate for Nogoya, both of which are much higher than we obtained from our samples (Table 1). These discrepancies could indicate sample heterogeneity in the sulfate distribution, as reported for carbonate abundances in these samples (e.g., Alexander et al., 2015). Alternatively, they could reflect the extraction of tochilinite (in which S is present as a sulfide) by Burgess et al. (1991) together with sulfate, as suggested by these authors. Tochilinite mineral could account for more than 50% of the S released at the temperature assigned for sulfate (Burgess et al., 1991), possibly explaining the roughly factor of two of difference between our data and the combustion data.

5.1.2. Elemental S

Burgess et al. (1991) report S^0 contents of 1500 ppm in Murchison, and 900 ppm for Nogoya using their stepped combustion approach. These values compare well with our extractions, being 1600 ± 100 ppm and 1400 ± 100 ppm S, respectively (Table 1). Note that Burgess et al. (1991) also reported 600 ppm S^0 for both Mighei and Murray, in the range of our CM extractions that averaged 1900 ± 1400 ppm S. Gao and Thiemens (1993) used CCl_4 as a solvent to extract S^0, and they report S^0 contents that were

typically <500 ppm S. We do not think that the higher S^0 contents we obtained compared to Gao and Thiemens (1993) results from an oxidation reaction during the extraction process (for instance from sulfide, or from an organic polysulfur compound). Our extractions were performed under anoxic conditions in an N_2atmosphere. We also note that water-soluble S-bearing organics would have been removed in the water traps before the S^0 extraction (Section 3.1). The discrepancy between our dataset and those of Gao and Thiemens (1993) therefore appears to be best explained by sample heterogeneity.

5.1.3. Sulfide

The extraction of sulfide was conducted with multiple steps. We first extracted the acid-volatile S fraction (AVS) by digesting the powdered samples in sub-boiling 6 N HCl. After the extractions, all the solutions displayed a yellow coloration, suggesting the presence of dissolved Fe^{3+}. Iron speciation is poorly characterized in CM, but Fe^{3+} is thought to be ubiquitous, hosted in magnetite and cronstedtite (e.g., Zolensky et al., 1997, Beck et al., 2012, Sutton et al., 2013, Howard et al., 2015). Reaction between reduced S and ferric iron can occur in acidic solution (Pruden and Bloomfield, 1968, Rice et al., 1993), producing S^0 as follows:

(1)$2Fe3++H2S \rightarrow 2Fe2++S0+2H+$

S^0 produced by reaction 1 can be recovered by the use of $CrCl_2$ solution (Canfield et al., 1986, Mayer and Krouse, 2004). We extracted the S^0 in solution (step 12) and the S^0fraction that had precipitated (step 13). Because S^0 is poorly soluble in acidic environments, S in step 13 is more abundant than in step 12. AVS represents only ~7% of the extracted sulfide pool, whereas steps 12 and 13 represent ~4% and ~89%, respectively. If correct, most of the sulfide is oxidized to S^0 during the AVS extraction, presumably due to the large Fe^{3+} contents in the studied samples. AVS $\Delta^{33}S$ values are compared to those of step 12 and step 13 in Fig. S2, and compared with the naturally occurring S^0 (i.e., step 2) in Fig. S3. The AVS, step 12 and step 13 isotopic compositions have, to first order, indistinguishable $\Delta^{33}S$ for most CMs (see detailed discussion in Appendix A). When compared with step 2, the data show considerable scatter, and do not fall on a 1:1 slope. Despite the lack of a clear $\delta^{34}S$ relationship, this further supports the conclusion that AVS, step 12 and step 13 are linked through sulfide oxidation during the AVS extraction (reaction 1). The differences between the step 2 and sulfide pools (Fig. S3) indicate that our protocol results in minimal contamination of the sulfide-derived S by the naturally occurring S^0.

5.1.4. Bulk S and sulfide contents of CMs: Comparison with previous work

Our observations suggest that most of the sulfide pool is oxidized during the AVS step and recovered in step 13. If not recovered properly, this might lead to an underestimation of both the sulfide content and the bulk S content of chondrites. We suggest that this accounts for the discrepancy between our study and Gao and Thiemens (1993) who reported bulk S contents for three CMs ⩽ 1 wt.%, ~75% of which is in sulfate. This is in contrast to the bulk S contents in our 13 CMs that range from 1.7 wt.% to 3.0 wt.%, with sulfide making up at least half the bulk S in most of them (Table 1). Gao and Thiemens (1993) recovered sulfide by digesting their chondrites in HCl, and only considered their AVS extractions as sulfide-derived S. Using this approach, <2000 ppm S from sulfide was extracted from each of their three CMs, compared to 8300–20,800 ppm in our study.

Burgess et al. (1991) and Dreibus et al. (1995) also determined S abundances in several CM falls. Burgess et al. (1991) reported an average S content of 2.99 ± 0.31 wt. % S (1σ) for four CMs (Murchison, Mighei, Nogoya, and Murray) and ranging from 2.65 wt.% to 3.38 wt.% S. Dreibus et al. (1995) report a comparable average bulk content of 3.26 ± 0.68 wt% (1σ) for eleven CMs, including three falls (Murchison, Cold Bokkeveld, and Nogoya) with individual bulk S contents varying between 2.20 wt.% and 4.90 wt.% S. Our bulk S contents for the same samples are lower by ~20–35%. Burgess et al. (1991) and Dreibus et al. (1995) both used combustion techniques and, therefore, likely accessed organic S. This could at least partially explain the differences in reported bulk S contents as only inorganic S was extracted with our protocol. Sulfur in soluble organic matter is likely to be <1% of the S budget (Cooper et al., 1997). The S content of insoluble organic matter is ~10 ± 5 wt.% (Alexander et al., 2007), representing ~0.1 wt.% S in the bulk rock or ~5% of the S budget in CMs. Thus, organically bonded S is only a partial explanation for the differences in bulk S contents reported here and the two earlier studies. If there were any sulfates that were insoluble in water (e.g., $BaSO_4$ and/or jarosite), these would not have been extracted by our protocol (Section 3.1). If so, the 20–30% lower S content associated with our technique relative to combustion studies (Burgess et al., 1991) would suggest that about half of the CMs sulfates would not be extracted by our technique. We cannot exclude this possibility, and systematic studies comparing bulk S data obtained by wet chemistry to combustion extractions on the same batches of powder are needed. Finally, sample heterogeneity is also a possible explanation, particularly when samples come from different stones of the same fall. Our replicate extractions on aliquots of the same Cold Bokkeveld and Murchison powdered samples yielded bulk S contents that varied by roughly a factor of 2 (Table 4). Bulk S contents reported by a number of other authors

also show factors of two variations for a given chondrite (Mason, 1963, Kaplan and Hulston, 1966, Jarosewich, 1971, Fitzgerald and Jaques, 1982, Kinnunen and Saikkonen, 1983, Graham et al., 1985). The only puzzle with this explanation is why, for the same meteorites, all our samples should have lower S contents than reported by Burgess et al. (1991) and Dreibus et al. (1995).

5.1.5. Sulfur isotope heterogeneity in different pieces of the Murchison meteorite

The comparison of our isotopic measurements of S from the British Natural History Museum sample of Murchison (BM.1988,M23) and the measurements by Gao and Thiemens (1993) (ME 2641) reveals a striking difference in the $\Delta^{33}S$ and provides evidence for significant S isotope heterogeneity in the Murchison material. This heterogeneity may reflect the fact that Murchison is a breccia containing xenolithic fragments of several other meteorite types, which are millimeter-to-centimeter-sized (e.g., Fuchs et al., 1973, Benedix et al., 2015).

For the Murchison splits reported by Gao and Thiemens (1993), all the S components have near zero $\Delta^{33}S$ values. In contrast, we observe strongly positive $\Delta^{33}S$ values in the three components extracted from our Murchison splits. It requires the redistribution of S-bearing phases along parent bodyprocesses (if any redistribution at all) to be limited to a scale below the meter scale (i.e. below what is sampled between Murchison rocks in different museums).

5.2. Exploring the genetic link between S^0 and sulfate

Based on their S isotopic composition, we develop the idea that sulfates in CMs result from parent body processing. The thermodynamic modeling of Zolensky et al. (1989) suggested that the Eh-pH conditions prevailing during aqueous alteration on the CM parent body would not allow for oxidation of sulfide to sulfate. However, Airieau et al. (2005) reported the occurrence of non-terrestrial $\Delta^{17}O$ for sulfate in 6 CMs falls (including Murchison, Cold Bokkeveld, Nogoya and Banten). This observation demonstrates that the sulfate formation occurred on the parent body, with extraterrestrial water, as opposed to sulfates forming on Earth.

If the only heated CM, PCA 91084, is excluded, sulfate has an average $\delta^{34}S$ of $-1.38 \pm 1.28‰$ (1σ, $n = 12$). This is systematically lower than the S^0 average of $3.56 \pm 0.74‰$ (1σ, $n = 12$ PCA 91084 excluded) or than the sulfide average of $-0.17 \pm 0.33‰$ (1σ, $n = 12$). Despite some overlap, the $\delta^{34}S$ of sulfate is generally lower than for sulfide, and is systematically lower than for S^0 in a given CM. Similar observations were made in the pioneering study of a single chip of Orgueil (CI) by Monster et al. (1965), as well as on Cold Bokkeveld, Mighei and Murray (Kaplan and

Hulston, 1966). Gao and Thiemens (1993) also report low $\delta^{34}S$ sulfate values relative to S^0 or sulfide in their CMs. If sulfates were formed by oxidation of a more reduced precursor (sulfide or S^0), these S isotope data would indicate an oxidation process that preferentially incorporates ^{32}S into the sulfate, producing isotopically light sulfate. This is consistent with a *normal* kinetic isotope effectassociated with oxidation like those that have been observed in the oxidation of aqueous sulfide (principally HS^-; e.g., Fry et al., 1988) and sulfide minerals (FeS; e.g., Lewis and Krouse, 1968).

Depending on the size of the studied reservoirs, resolvable ^{34}S enrichments are expected in the residual precursor. Sulfate represents on average 25 ± 12% of the bulk S whereas sulfide and S^0 represent 65 ± 15% and 9 ± 7% respectively (Section 4.2). Assuming closed system (Bland et al., 2009) and that the sulfate precursor (sulfide or S^0) had a $\delta^{34}S$ equal to CDT, the roughly 1‰ ^{34}S-depletion in sulfate relative to CDT should be compensated by a roughly 0.4 or 2.5‰ ^{34}S-enrichment in the sulfide or S^0 pool, respectively. Sulfide and S^0 have average $\delta^{34}S$ values of −0.15 ± 0.33‰ and +3.46 ± 0.74‰ (1σ), respectively. Within uncertainty, both mechanisms could be reasonable explanations, and on the basis of this ^{34}S mass balance, sulfate could be formed by both oxidation of sulfide or S^0.

Sulfates in chondrites could have been produced on Earth, by reaction of sulfides (and/or elemental S) with atmospheric oxygen. For example, Gounelle and Zolensky (2001) report clear evidence for sulfate veins formation in Orgueil (CI chondrite) during the storage history of the samples. This is consistent with the Orgueil sulfate $\Delta^{17}O$ value of −0.12 ± 0.20‰ (2σ, Airieau et al., 2005), i.e. indistinguishable from sulfates formed on Earth (with a $\Delta^{17}O$ value of 0.00‰, Airieau et al., 2005). This could indicate that mostly terrestrial oxygen was involved in the formation of these sulfates (Airieau et al., 2005). On the other hand, CMs have sulfate with variable $\Delta^{17}O$ values, between +1.18 ± 0.20‰ and −0.23 ± 0.20‰. These values are clearly not terrestrial, indicating that sulfates in CMs, in contrast to CIs, were mostly produced in their parent body during late stage aqueous alteration (Airieau et al., 2005). Interestingly, the bulk $\Delta^{17}O$ values for CMs is between −0.67‰ and −3.07‰ (Clayton and Mayeda, 1999), always significantly lower than the corresponding sulfate values (Airieau et al., 2005). In the canonical water/rock interaction model (Clayton and Mayeda, 1999), this would indicate that the sulfates were produced early in the aqueous alteration sequence, before substantial isotopic exchange between water (presumably carrying a high $\Delta^{17}O$ value) and the anhydrous silicates (presumably carrying a low $\Delta^{17}O$ value) had occurred (Clayton and Mayeda, 1999).

Independent of when and where the chondritic sulfates were produced, the question of their precursor (sulfide, S^0, or another S-bearing phase) remains elusive, at best, in the literature. Petrographic analyses of CMs report alteration of sulfides (e.g., Zolensky et al., 1997, Rubin et al., 2007), suggesting that sulfide oxidation will contribute to the chondritic sulfate budget. However, sulfates always display $\Delta^{33}S$ anomalies that are significantly larger than sulfide (Fig. 7). Since sulfide oxidation would only transfer the sulfide $\Delta^{33}S$ to the sulfates, the mismatch between sulfates and sulfides $\Delta^{33}S$ values indicate that sulfides cannot be the main precursor of sulfate. On the other hand, sulfate and S^0 have similar $\Delta^{33}S$ values (Fig. 7). The slope observed between $\Delta^{33}S$ values of S^0 and sulfate is 0.86 ± 0.24 (2σ) with an intercept of 0.028 ± 0.018‰. At first order, this slope is statistically indistinguishable of a 1:1 slope, allowing sulfate to be produced by S^0 oxidation, not sulfide oxidation. This is not true for the sulfates from MCY 02530 that have a $\Delta^{33}S$ value that is indistinguishable from the sulfides of this CM, and significantly different from that of S^0. This CM is excluded from the following discussion.

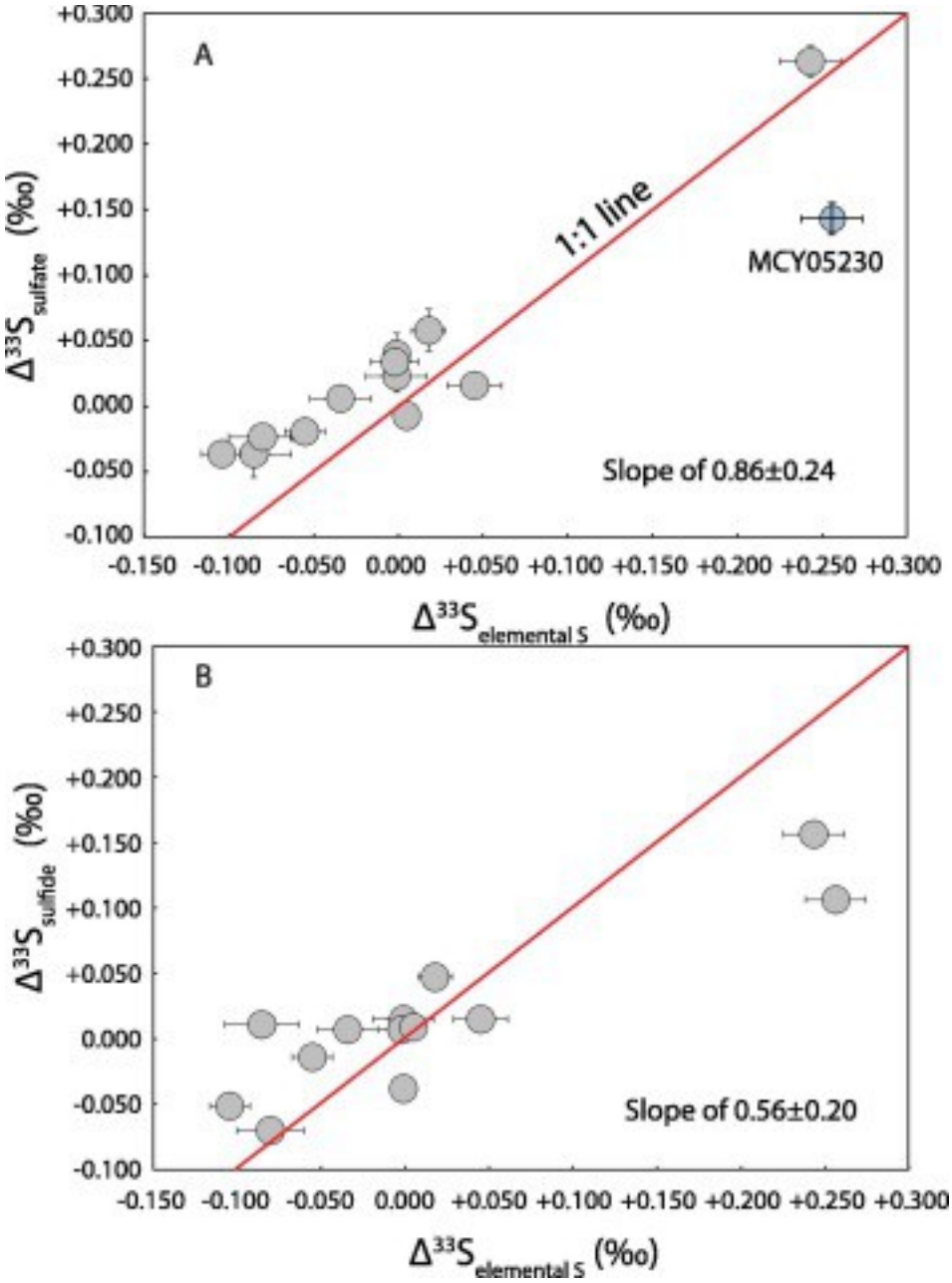

1. Download high-res image (264KB)
2. Download full-size image

Fig. 6. An evaluation of the genetic links between the S-carrying phases in CMs. The $\Delta^{33}S$ values of S^0 are plotted against (a) the sulfate, and (b) the sulfide values. The 1:1 slopes are shown in red. The S^0-sulfate trend is indistinguishable from a 1:1 slope (MCY 05230 is excluded). For all CMs except MCY 05230, this suggests a direct link between sulfate and S^0 (see Section 5.2). Sulfide and S^0may be linked through their condensation sequence or via the delivery of late sulfide to the CMs that partially oxidize to S^0 (see

Section 5.4). (For interpretation of the references to colour in this figure legend, the reader is referred to the web version of this article.)

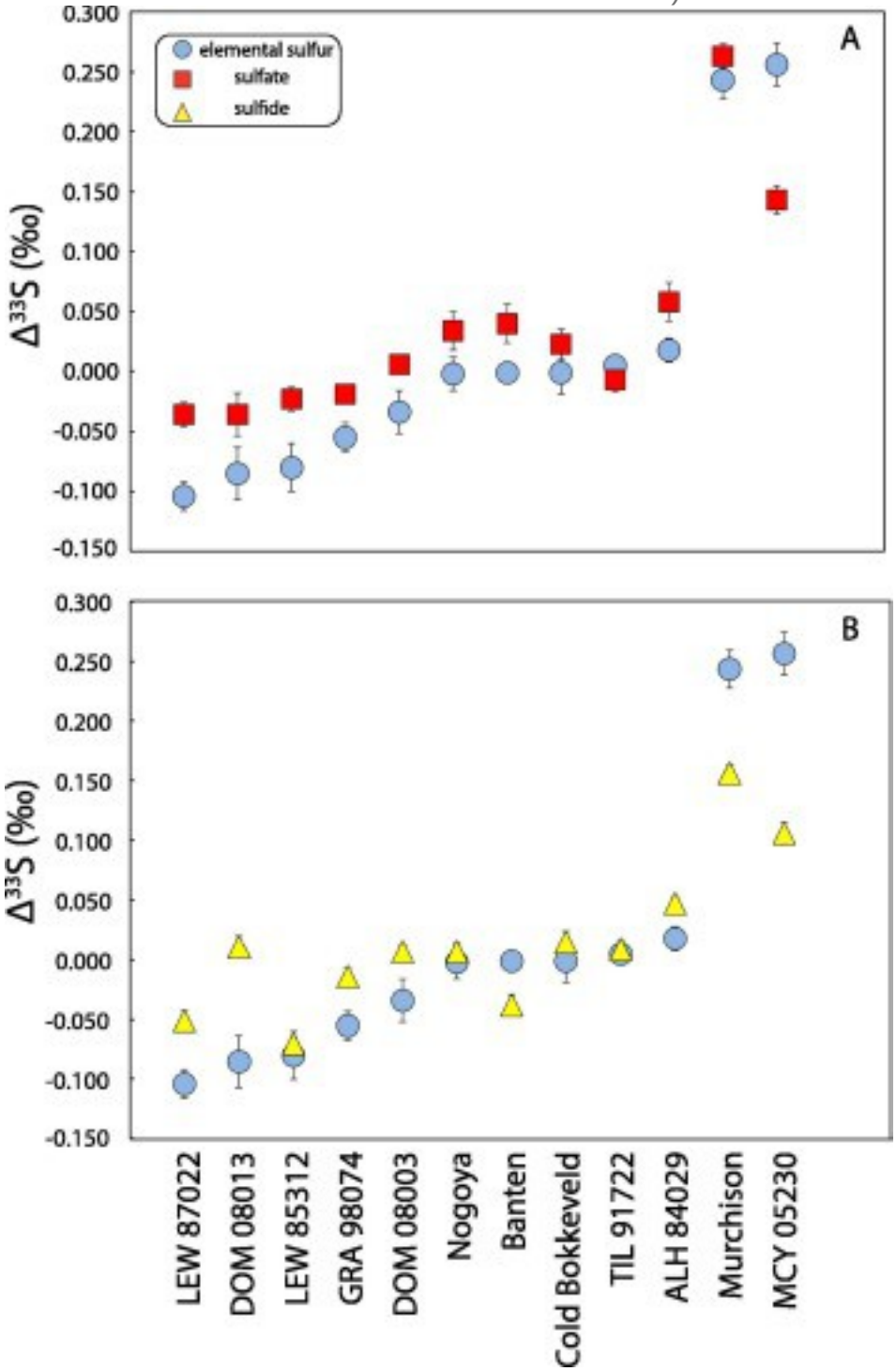

1. Download high-res image (246KB)
2. Download full-size image

Fig. 7. The $\Delta^{33}S$ values of S^0, sulfate and sulfide, in 12 CMs (PCA 91084, the only heated CM, is excluded). The isotope data are given relative to CDT. Chondrites are ranked by order of increasing $\Delta^{33}S$ values in S^0. The values for S^0 are compared with (a) sulfate and (b) sulfide.

Although sulfates and S^0 have similar $\Delta^{33}S$ values, sulfates always seem to be biased toward slightly higher $\Delta^{33}S$ values than S^0 at the ~0.020–0.060‰ level (averaging at +0.036 ± 0.042‰, 2σ, versus a total range of ~0.300‰). This is evident in Table 3, Figs. 7A and 9. This slightly higher $\Delta^{33}S$ value in sulfate, relative to S^0, is correlated to the ^{34}S difference between sulfate and S^0: The more sulfates are depleted in ^{34}S relative to S^0, the higher their $\Delta^{33}S$ are relative to S^0 (Fig. 9). In addition, sulfates show a slight $\Delta^{36}S$ depletion relative to S^0, averaging at −0.31 ± 0.26‰ (2σ). However, the relative $\Delta^{36}S$ uncertainties are significantly larger than for $\Delta^{33}S$ (Table 3), preventing any direct trend with $\delta^{34}S$ values to be observed (Table 3). This is nevertheless the first time that the relationship observed in Fig. 9 is observed in natural samples, and we suggest that it reflects the specific nature of the S^0 oxidation mechanism to sulfate. The mass dependence of an isotope fractionation accompanying a chemical reaction or physical process among more than two stable isotopes is typically given by a power law relationship, e.g., $^{33}\alpha = (^{34}\alpha)^{\theta}$ where α is the fractionation factor (Craig, 1957, Hulston and Thode, 1965, Matsuhisa et al., 1978, Clayton and Mayeda, 1996, Young et al., 2002). By convention, the reference exponent θ for the relationship between $^{33}\alpha$ and $^{34}\alpha$ is taken to be 0.515, the approximate exponent of mass dependence describing most simple equilibrium isotope exchange reactions (Matsuhisa et al., 1978, Young et al., 2002). Rare exceptions to this rule have been observed, particularly for complex kinetic processes, where exponents of mass dependence differing significantly from the reference exponent of 0.515 were observed and coined “non-canonical” effects (Eiler et al., 2013). For those fractionations, $\Delta^{33}S$ is predicted to depart from a reference across a given process and to be correlated with $\delta^{34}S$ variations. In our case, a mechanism linking S^0 and sulfate would require that the $^{33}S/^{32}S$ fractionation be 0.505 ± 0.005 times that of the $^{34}S/^{32}S$ fractionation.

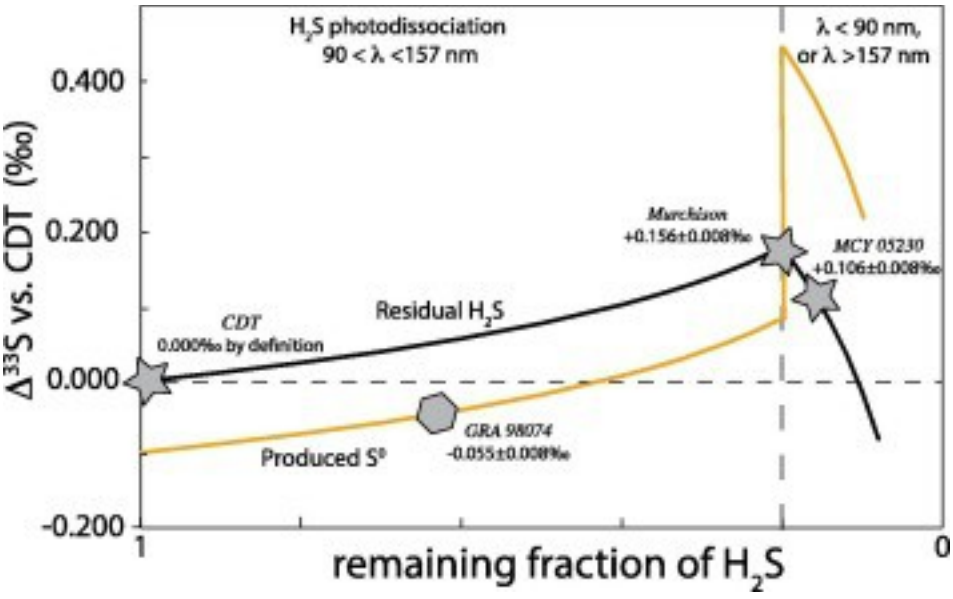

1. Download high-res image (156KB)
2. Download full-size image

Fig. 8. Schematic representation of the H_2S photodissociation under open-system Rayleigh distillation conditions as described in model A (see Section 5.4.1.). The *x*-axis is the remaining fraction of H_2S in the nebula. The *y*-axis is $\Delta^{33}S$, shown for the remaining H_2S and the instantaneous product S^0. The star symbols are used for illustrating the composition of H_2S. The composition of the initial H_2S reservoir and H_2S likely recorded by Murchison and MCY 05230 sulfide pools are shown. The hexagon symbol is used for illustrating the composition of produced S^0 for GRA 98074 as an example (Section 5.4.1). For the first and second photodissociation regime ($f > 0.2$ and $f < 0.2$, respectively), $\Delta^{33}S$ fractionations are taken at −0.1‰ and +0.3‰, respectively. For most CMs, $\Delta^{33}S$ values of S^0 are lower than for sulfide, as accounted for by the first photodissociation regime. Additionally, it corresponds to $\Delta^{36}S/\Delta^{33}S$ values for CMs at −3.1 ± 1.0, consistent with H_2S photodissociation occurring at λbetween 120 and 139 nm. The one example of GRA 98074 is taken for illustration here. The conclusion does not change if other CMs were taken for illustration (Section 5.4.1). For Murchison and MCY 05230, the $\Delta^{33}S$ values of S^0 are higher than for sulfide, and the $\Delta^{36}S/\Delta^{33}S$ values are positive, indicating a change in the main wavelength responsible for the photodissociation (Sections 5.4.1. and 5.4.2). The minimum $\Delta^{33}S$ value of H_2S at the transition between the two regimes requires a low *f* value (here 0.2) as constrained by the Murchison value of +0.156 ± 0.008‰. This requires substantial processing of H_2S for its isotopic composition to have evolved significantly from CDT. We suggest here that the photodissociation process recorded by Murchison and MCY 05230 could postdate the recorded in the other chondrites studied here. Note that with a $\Delta^{36}S/\Delta^{33}S$ of ∼−3, the first photodissociation regime would lead the $\Delta^{36}S$ values for Murchison and MCY 05230

to be −0.45 ± 0.30‰, which is not seen (these CMs have $\Delta^{36}S$ values closer to zero, Table 3). Although the large uncertainties on $\Delta^{36}S$ values for these two CMs do not allow invalidating the present prediction, a preferred alternative model is developed in Section 5.4.3.

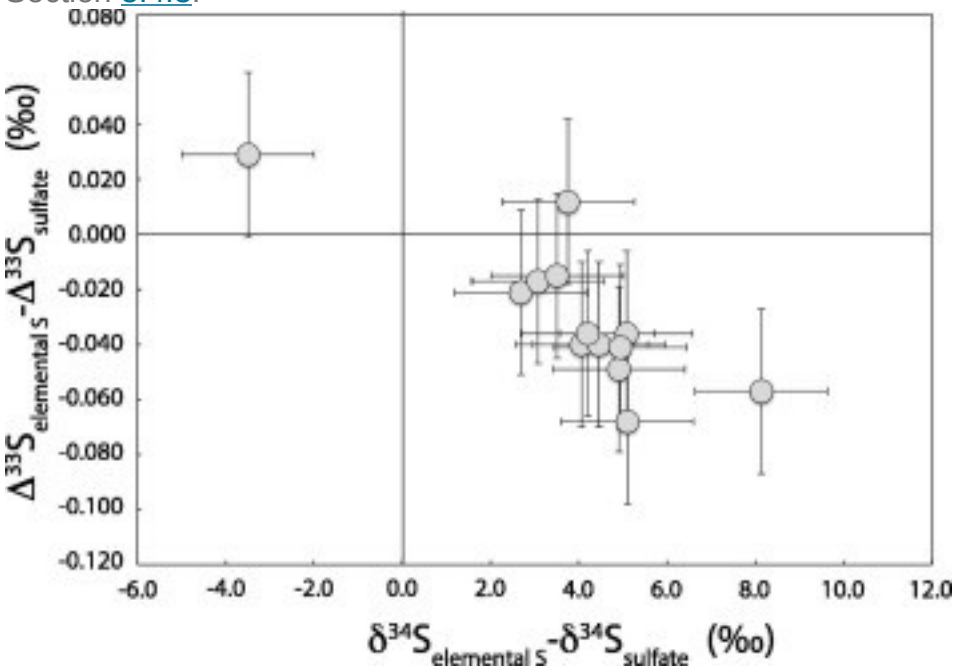

1. Download high-res image (117KB)
2. Download full-size image

Fig. 9. The S isotopic relation between sulfate and its potential precursors: S^0 and sulfide. (a) The $\delta^{34}S$ difference between sulfate and S^0 is plotted versus their $\Delta^{33}S$ difference. (b) The difference between sulfate and sulfide. The occurrence of at least three outliers in the trend between sulfate and sulfide argues against a direct genetic link between sulfate and sulfide. There is a direct negative trend between S^0 and sulfate. This suggests a sulfate origin through S^0 oxidation in the CM parent body (see also Fig. 6). The ^{34}S depletion in sulfate, relative to S^0, indicates that the oxidation process is a normal kinetic mechanism. The more sulfates are depleted in ^{34}S relative to S^0, the higher their $\Delta^{33}S$ are relative to S^0. We estimate that the $^{33}S/^{32}S$ fractionation is 0.505 ± 0.005 times that of the $^{34}S/^{32}S$ fractionation. As observed for the first time in natural samples, this relationship indicates that the kinetic oxidation process is characterized by a non-canonical mass dependency (see details in Section 5.2).

5.3. Sulfur cosmochemistry

The analyses presented here yield a much larger range of S-MIF in the major S-carrying phases than previously recognized in chondrites. Gao and Thiemens (1993) may have missed identifying the signature because the number of CM chondrites that they studied

was small (n = 3). Repeat analyses of the same meteorites in some cases match well within uncertainty with Gao and Thiemens (1993), but we report a distinctly different bulk S isotope composition for Murchison, suggesting sample heterogeneity. The largest S-MIF signals are found in S^0, but they are also preserved in sulfide and sulfate – the latter being a water-soluble phase.

Mixing of S from diverse nucleosynthetic origins, such as that associated with ^{32}S-bearing SiC attributed to decay of ^{32}Si produced in supernovae, is not a good mechanism for explaining the observed S isotope anomalies in CMs. SiC grains comprise 30 ± 15 ppm of CMs (Davidson et al., 2014), and of these, the grains carrying ^{32}S-excesses ($\Delta^{33}S$ values down to −500‰) are rare (~1–5% – Hoppe et al., 2012, Fujiya et al., 2013, Pignatari et al., 2013). Considering the S abundance of CMs, ^{32}S addition by these grains would only raise the $^{32}S/^{34}S$ ratio by $\sim 5 \times 10^{-5}\%$, ~3 to 5 orders of magnitude too low to account for the $\Delta^{33}S$ variations in S^0 and sulfide, respectively.

The significant non-mass dependent (>0.1‰) ^{33}S variations in phases that condense at different temperatures suggest a photochemical process. During its T-Tauri phase, the young Sun would have emitted significantly greater deep and extreme UV than it does today (Zahnle and Walker, 1982). This UV radiation would have been available for photolysis in the transparent hotter inner parts of the solar nebula (Rai et al., 2005) and along unshaded parts of the surface of the disk, as modeled by Ciesla (2010) and Ciesla and Sandford (2012). Any produced photochemical S-isotopic signature could have been transferred to solids via condensation of S-bearing phases, followed by transportation to the midplane of the disk by vertical mixing (Ciesla, 2010) where it would have been accreted as part of the chondrite matrices.

For the present CM S isotope data, the carrier of the anomaly appears to be related to S^0 or an S^0-precursor rather than a high temperature sulfide condensate, as was suggested in prior studies (Rai et al., 2005, Rai and Thiemens, 2007, Antonelli et al., 2014), but the production mechanisms of the S^0 or S^0-precursor remains unclear. The S-MIF signature could reflect direct photochemical production of S^0, provided that sufficient UV were available in the cooler parts of the disk where S^0 could condense or be captured by grain surfaces.

The observation that $\Delta^{33}S$ values of S^0 (which is water-insoluble) is correlated with values in water-soluble phases (such as sulfate), in combination with the observation that different pieces of the same meteorite preserve evidence for variable $\Delta^{33}S$ values (Murchison) implies that the S-MIF signal is variable on a sub-meter scale at least in Murchison. The corollary is that parent body aqueous processing and flow was not

sufficient to homogenize the isotopic signals at this scale. This argues against a pervasive fluid flow in the regions where the CM chondrites were formed.

PCA 91084, the only heated CM analyzed here (Alexander et al., 2007, Alexander et al., 2013), displays a S chemistry pattern that differs from the other CMs. We suggest that this may reflect oxidation during heating in the CM parent body (Appendix B). Further study of heated carbonaceous chondrites is needed to validate this hypothesis.

5.4. H_2S Photochemistry as a candidate production mechanism for S-MIF

H_2S photochemistry is considered as a candidate for the S-MIF production because it is thought to be the dominant S-bearing gas phase in the solar nebula (e.g. Chakraborty et al., 2013, Pasek et al., 2005). H_2S absorbs in several regions in the UV, with a broad absorption feature extending from ~317 nm to ~165 nm, and a series of banded absorption features that extend from ~165 nm down to ~40 nm with a peak at ~90 nm. This peak includes several bands around Lyman alpha wavelengths at 121.6 nm (i.e., the most intense T-Tauri wavelengths, Zahnle and Walker, 1982, Okabe, 1978). The longer wavelength feature appears to be associated with the production of atomic hydrogen and SH, while the shorter wavelength region is associated with the production of atomic H and S (Okabe, 1978).

Farquhar et al. (2000b) report isotopic fractionationsassociated with photolysis experiments that access the longer wavelength (~317 nm to ~165 nm) absorption feature using continuum radiation extending from ~200 nm to the visible. Recently, Chakraborty conducted a series of photolysis experiments of H_2S by UV radiation with wavelengths of 90, 121.6, 139.1, and 157 nm to investigate isotope effects in the shorter wavelength region. These experiments indicate that photolysis at different wavelengths produces S^0 and residual H_2S with different types of isotopic signals, most notably $\Delta^{36}S/\Delta^{33}S$ ratios that vary as a function of the wavelength of the incident UV. The experiments undertaken by Farquhar et al. (2000b) yielded positive $\Delta^{33}S$ values in the produced S^0, where products and residues lie on a positive $\Delta^{36}S/\Delta^{33}S$ array (~+1.7 ± 1.5, 2σ, see Farquhar et al., 2000b). On the other hand, the photolysis experiments of Chakraborty et al. (2013)undertaken at discreet wavelengths of 122 nm and 139 nm produced negative $\Delta^{33}S$ values in S^0 down to −1.54 ± 0.02‰, and a $\Delta^{36}S/\Delta^{33}S$ ratio of −2.77 ± 0.46 (2σ). Experiments conducted at 90 nm and 157 nm yielded S^0 with positive $\Delta^{33}S$ values and near-zero $\Delta^{36}S$ values, yielding $\Delta^{36}S/\Delta^{33}S$ values of +1.4 ± 0.2 and +0.1 ± 0.2, respectively (Chakraborty et al., 2013). Note that there are no systematic $\delta^{34}S$ variations between the different mass independent signatures in the experiments (Chakraborty et al., 2013). Thus, as opposed to non-canonical mass dependant

fractionations (Section 5.2, Eiler et al., 2013), no systematic $\delta^{34}S$ variations can be *a priori* expected to correlate with the MIF signatures.

In CMs, most S^0 extracts have homogeneous $\delta^{34}S$, negative $\Delta^{33}S$ values and lie on a $\Delta^{36}S/\Delta^{33}S$ slope of −3.1 ± 1.0 (−3.9 ± 2.2 when sulfide and sulfate extracts are taken into account; 2σ; Figs. 4a and 5). This relationship is similar to that seen in the experimental results in the Lyman alpha region (Chakraborty et al., 2013). Given that this is one of the most intense emission regions in the far ultraviolet of T-tauri stars(Zahnle and Walker, 1982) we suggest a link to the observation of S-MIF in the CM chondrites.

The positive $\Delta^{33}S$ values for S^0 of Murchison and MCY 05230 are associated with near-zero $\Delta^{36}S$ values, or $\Delta^{36}S/\Delta^{33}S$ values of +0.9 ± 0.1 and +1.3 ± 0.1, respectively, suggest a different mechanism. Magnetic isotope effects, producing large $\Delta^{33}S$ anomalies associated with negligible $\Delta^{36}S$ variations, could explain these values. It was experimentally shown that S magnetic isotope effects can be produced in highly specific chemical conditions during S reductionprocesses (Oduro et al. 2011). This process leads to the preferential partitioning of ^{33}S into the products of the reaction (sulfides), leaving behind ^{33}S-depleted sulfates. In the CMs the sulfates, sulfides and S^0 all share positive $\Delta^{33}S$ anomalies, leaving unexplained what the complement of these isotopic reservoirs would be. It is also unclear why only two of the CMs would have experienced processes allowing the expression of magnetic isotope effect, without affecting any other meteorites. We here argue that the positive $\Delta^{36}S/\Delta^{33}S$ ratios can also result from a photodissociation process, since several H_2S photodissociation experiments show positive $\Delta^{36}S/\Delta^{33}S$ ratios, including those conducted at both shorter and longer wavelengths than the Lyman alpha wavelengths (Chakraborty et al., 2013). Considering that absorption by gas phase species such as H_2, CO, CH_4, N_2, NH_3 would preferentially shield shorter wavelengths (Keller-Rudek et al., 2013), we suggest this change reflects a shift to longer wavelengths after attenuation of Lyman alpha by absorption in the nebula (See Fig. 8). Importantly, variations of $\Delta^{36}S/\Delta^{33}S$ from sample to sample (Fig. 5) resulting from the photodissociation processes provide evidence for heterogeneous accretion of S-bearing phases by the parent body of CMs. This rules out parent body processes as the cause for these S isotope variations (through for example the heterogeneous redistribution of some S-MIF-bearing phase *after* accretion).

5.4.1. Model A: sulfides and S^0 are both direct condensates

One possibility for explaining the S isotope variations in CMs is that when temperatures in the nebula were low enough, any photolytic S^0 carrying S-MIF condensed and the remaining H_2S sulfidized metal to form sulfides following reaction 2(Zolensky and Thomas, 1995, Lauretta et al., 1996, Lauretta et al., 1997).

(2)Fe0+H2S=FeS+H2

Metal sulfidation experiments show that the reaction 2 leads to the formation of troilite (FeS) at ~700 K (Lauretta et al., 1996). At a given H_2S content, the sulfidation rate decreases dramatically with temperature, but this mechanism remains efficient until temperatures are as low as ~500 K. Negative $\Delta^{33}S$ values in S^0 are predicted to be associated with positive $\Delta^{33}S$ values in H_2S (recorded in sulfides), by mass balance, as observed in H_2S photodissociation experiments (Chakraborty et al., 2013). Negative trends between $\Delta^{33}S$ values for S^0 and sulfides are hence predicted. However, a clearly positive trend is observed, with a slope of 0.56 ± 0.20 (2σ, Fig. 6b). H_2S photodissociation associated with an open-system Rayleigh distillation process can reconcile the data with the experiments: Any S^0 would carry a negative $\Delta^{33}S$ value relative to the residual H_2S, without a significant change in $\delta^{34}S$ (Chakraborty et al., 2013). In an open-system model, the photolytic S^0 would be distilled out of the system by condensation, continuously or in discreet episodes, and deposited without substantial accumulation in the chondritic matrices. This would enrich both the produced S^0 and the remaining H_2S in ^{33}S. Assuming a bulk solar composition of $\Delta^{33}S = 0$, Rayleigh distillation is required to account for the occurrence of both positive and negative $\Delta^{33}S$ values for $S^0$and sulfides (Fig. 8), as well as the observed positive correlation between sulfide and S^0 (Fig. 6b). Photolytic processes producing S-MIF under a Rayleigh distillation have been suggested elsewhere, as to occur in the Earth's upper atmosphere for SO_2 photodissociation, explaining the S isotopic composition of sulfate deposits in volcanic ashes from Antarctic ices (Baroni et al., 2007).

Quantitative modeling of S^0 abundances and isotopic compositions in CMs remains challenging: Experiments for H_2S photodissociation at 121.6 nm and 139.1 nm yielded $\Delta^{33}S$ fractionations between produced S^0 and residual H_2S ranging between −1.54 ± 0.02‰ and −0.09 ± 0.02‰ without systematic changes in $\delta^{34}S$ (Chakraborty et al., 2013). A Rayleigh process involving these isotopic fractionations could have produced the fractionations seen in all of the CM chondrites except Murchison and MCY 05230. For the sake of illustration, we model an endmember case with constant $\Delta^{33}S$ fractionations and negligible $\delta^{34}S$ fractionations (Fig. 8). The $\Delta^{33}S$ values for S^0 in CMs range between −0.107 ± 0.008 and +0.045 ± 0.008‰, which are consistent with a model where chondrites sampled S^0 produced by a Rayleigh process with a −0.1‰ $\Delta^{33}S$ S^0-H_2S fractionation during H_2S photodissociation. If reaction 2 is ignored, the calculation yields a fraction of remaining H_2S (*f*) between 0.99 and 0.30 to account for the range of S^0 isotopic compositions in all the CMs except Murchison and MCY 05230 (Fig. 8). Note that the *ad hoc* −0.1‰ value for the fractionation is consistent with the ~0.1 ± 0.1‰

difference generally observed between S^0 and sulfide in the CMs (Table 3). A larger magnitude fractionation would reduce the required *f* range needed to reproduce the data. Using a fractionation of −1.5‰ would require an $f < 0.4$ to satisfy the observations, and all S^0 produced for $f > 0.4$ would have been lost.

CMs would be required to sample S^0 that underwent likely <10% incremental accumulation after its production, consistent with S^0 being the smallest S reservoir in the CMs (Table 2). The amounts of S^0 produced could be calculated after determining *f* values for each chondrite. For example, GRA 98074 displays a $\Delta^{33}S$ value of −0.055 ± 0.008‰ for S^0, which would correspond to an instantaneous product at a fraction of residual H_2S (*f*) of 0.65 (Fig. 8). This isotopic value could also be produced by accumulation of all S^0 for *f* values ranging between 0.7 and 0.6 (Fig. 8) or between 0.66 and 0.64. The trade-off between these possibilities is dictated by the acceptable amount of S^0 accreted in this chondrite to match the measured S^0 content (1000 ± 100 ppm S for GRA 98074, Table 2). For ALH 84029, its S^0 content is 5500 ± 100 ppm with a $\Delta^{33}S$ value of +0.018 ± 0.008‰ (Table 2, Table 3). This $\Delta^{33}S$ value would be reached for $f \approx 0.3$, but the higher S^0 content would require more S^0 accumulation. However, because the relative rate of photodissociation ($H_2S \rightarrow S^0 + H_2$, Fig. 8) to sulfidation ($H_2S + Fe^0 = FeS + H_2$, reaction 2) is unknown, *f* values cannot be translated into S^0concentrations. Nonetheless, this simple model qualitatively accounts for the absence of direct trend between the S^0isotopic composition and the amount of S^0 observed in a given CM (Table 2, Table 3).

The distinct $\Delta^{36}S/\Delta^{33}S$ values for Murchison and MCY 05230, relative to all other CMs, require a change of the photodissociation regime across the S condensation window (Section 5.4). This is also consistent with the reversal of the $\Delta^{33}S$ difference between S^0 and sulfide for these two CMs (Table 3 and Fig. 8). In this context, the positive $\Delta^{33}S$ values of both S^0 and sulfide in the two meteorites could be explained if these phases were derived from a S reservoir that had already acquired a ^{33}S enrichment. One could speculate that the first photodissociation regime (with $\Delta^{36}S/\Delta^{33}S \sim -3$ and producing increasing $\Delta^{33}S$ values with decreasing *f* values, Fig. 8) was responsible for the ^{33}S enrichment. In that case, the minimum $\Delta^{33}S$ value of H_2S at the transition between the two regimes would be constrained by the Murchison sulfide value to be at least +0.156 ± 0.008‰. Fig. 8 illustrates the endmember possibility where the first regime ($\Delta^{36}S/\Delta^{33}S \sim -3$) is recorded by most of the CMs, while a second one accounts for Murchison and MCY 05230 only, with a $\Delta^{33}S$ fractionation of +0.30‰. Considering the $\Delta^{33}S$ value of +0.156 ± 0.008‰ and a $\Delta^{36}S/\Delta^{33}S$ of ∼−3, the first photodissociation regime would lead the $\Delta^{36}S$ values for Murchison and MCY 05230 to be −0.45 ± 0.30‰.

These two CMs however have near-zero $\Delta^{36}S$ values with only marginal overlap with this prediction (Table 3). While the uncertainties on $\Delta^{36}S$ do not allow us to completely rule out this possibility, below we develop an alternative and preferred model where the isotopic signatures seen in sulfide and S^0 could derive from a common product that contaminated both components. We discuss this interpretation later in this communication.

5.4.2. Other implications and limitations

This model requires both S^0 condensation and FeS formation to occur *coincident with* the photodissociation process. Under canonical nebula conditions, the rate of FeS formation reaction (reaction 2) would have been highest at ~700 K (Lauretta et al., 1996, Lauretta et al., 1997), but non-negligible until temperatures fell below ~500 K (Lauretta et al., 1996, Lauretta et al., 1997, Llorca and Casanova, 2000). Experimental data suggest a likely sublimation temperature of S^0 allotropes <370 K, although the only available data were obtained at 1 bar and under O_2-bearing atmospheres (Meyer, 1976 and references therein). If relevant to canonical nebular conditions ($P \sim 5 \times 10^{-4}$ bars, with solid grains in suspension), this is below the minimum FeS formation temperature, and would argue against this working hypothesis. Note that we remain cautious about ruling out such a sink for S^0 because it is unclear whether photochemical production of S intermediates that have an affinity for grain surfaces could play a role in sequestering some anomalous S at temperatures above the sublimation temperature of S^0.

In this model, chondrites sample snapshots of the S^0produced by H_2S photodissociation under a Rayleigh distillation process. While qualitative inferences about the process appear possible, quantitative modeling of S^0abundances and isotopic compositions in CMs has not been attempted as $\Delta^{33}S$ fractionations vary as a function of wavelength without producing systematic $\delta^{34}S$ variations (Chakraborty et al., 2013). We illustrate a simple scenario in Fig. 8 using prescribed fractionations, but do not address the issue of incident wavelength or the relationship between isotopic composition and mass balance because the relative rate of photodissociation to sulfidation is unknown. A point in favor of the general Rayleigh model approach is that the range of $\Delta^{33}S$ anomalies, from significantly negative to positive values, is consistent with a Rayleigh distillation mechanism, accompanied by inefficient accretion of S^0 in CM matrices as suggested by S^0 being the smallest S reservoir (Table 2).

Model A predicts that the CM with the lowest S^0 $\Delta^{33}S$ value will have a sulfide value that is closest to the bulk composition of the gas (Fig. 8). This is LEW 87022 with a value of

−0.104 ± 0.012‰ for S^0, and −0.051 ± 0.008‰ for sulfide (Fig. 7B). The bulk $\Delta^{33}S$ value of the nebula would be between these two values (but probably closer to −0.051 ± 0.008‰, Fig. 8), i.e., clearly distinct from CDT. This would leave unexplained the observation that only rare differentiated bodies show significantly negative $\Delta^{33}S$ values. While the mantles of the Earth, Mars, and the Moon have near-CDT $\Delta^{33}S$ values, only subgroups of irons display negative $\Delta^{33}S$ values, with an average $\Delta^{33}S$ value of −0.027 ± 0.008‰ for IIIF (Labidi et al., 2013, Franz et al., 2014, Antonelli et al., 2014, Wing and Farquhar, 2015). If the H_2S in the CM formation region had a CDT-like S isotope composition to begin with, the model fails to explain the isotope composition of LEW 87022.

5.4.3. Model B-1: S-MIFs in chondrites are brought to the CMs by ice accretion

A second working hypothesis posits that at T > 500 K, the S^0vapor produced by photodissociation of H_2S would not condense and be rapidly removed by reaction with H_2 to form H_2S since H_2 is the main gas in the nebula (Lodders, 2003), as follows:

(3)S0+H2=H2S

Under this hypothesis, the transfer of S-MIF to sulfide precursors, and ultimately to iron sulfides would be prevented. Some H_2S probably remained in the nebula after troilite formation (T < 500 K), accounting for the S content of Jupiter atmosphere (Gautier et al., 2001, Ciesla, 2015). Under this hypothesis, residual H_2S when subjected to UV irradiation at T < 500 K would yield S^0 that eventually would be allowed to condense. The variable $\Delta^{33}S$ values in sulfides positively correlated with the S^0 values (Fig. 6b), though, would require some transfer of the MIF carried by S^0 to the sulfides. However, evidence exists only for sulfide oxidation in chondrites, not S^0 reduction (e.g., Kerridge et al., 1979, Zolensky et al., 1997, Gounelle and Zolensky, 2001, Bullock et al., 2005, Bullock et al., 2010).

Accretion of ices to the CM matrices could provide a mechanism for transferring S-MIF in both sulfides and S^0, under this working hypothesis. Late-accretion of nebular S^0itself by ices is seen as unlikely, as experimental data suggest that it is significantly more refractory than water under any conditions, and hence it is likely to have condensed from the gas phase well before water ice formation (Jiménez-Escobar and Caro, 2011). As an alternative, ice accretion could deliver the remaining H_2S (freezing T < 170 K, Jiménez-Escobar and Caro, 2011) to the CM matrices. In support of this idea, comets have been observed to host a variety of S-bearing molecules, H_2S being the dominant one, representing from 0.2 to 1.5% relative to H_2O (Irvine et al., 2000). This H_2S gas would carry S-MIF after partial photodissociation in the nebula

at T < 500 K. Its release in the CM parent body during aqueous alteration would have allowed reaction 1 to occur: H_2S would have reacted with Fe^{3+} present in the aqueous fluids that was produced by metal oxidation (Zolensky et al., 1997, Beck et al., 2012, Sutton et al., 2013, Howard et al., 2015). This reaction, commonly observed in the laboratory (Section 5.1.3), would lead to the formation of S^0 with S-MIF. Observations of the least altered CM meteorite Paris supports the idea that metal would have been available in the first alteration reactions (Hewins et al., 2014). Therefore, the reaction 2 could also occur on the parent body. The competition between the reactions (1), (2) would have led to the formation of S^0 (reaction 1) as well as a second generation of sulfides (reaction 2), both bearing identical $\Delta^{33}S$ values. It is conceivable that such a process would have resulted in the further sulfidation of troilite, leading to formation of pyrrhotite(Zolensky and Thomas, 1995). Regardless, because our extraction process cannot distinguish between the primary sulfides (CDT-like $\Delta^{33}S$ values) and the S-MIF bearing sulfide formed by reaction 2, this scenario would predict bulk sulfides $\Delta^{33}S$ values that are correlated with the values for S^0, which consistent with our dataset (Fig. 7b).

5.4.4. Model B-2: S-S production resulting from ice irradiation

A variant of this working hypothesis relates to UV irradiation of H_2S-bearing ices. Multiple lines of experimental evidence show that various S^0 species are produced by the irradiation of H_2S ices by UV (or protons) under relevant nebular conditions (Jiménez-Escobar and Caro, 2011, Moore et al., 2007). As H_2S being in a solid (icy) state, it is not known whether its photodissociation would generate a mass-independent anomaly. We note though that the UV irradiation process of the ices in the protoplanetary nebula can be associated with warming of the ices, leading to temperatures allowing H_2S desorption (Ciesla and Sandford, 2012, Jiménez-Escobar et al., 2014). This would allow the photodissociation to have occurred under gas state, leading to production of S-MIF (Chakraborty et al., 2013). If products recondensed on ice, this mechanism could constitute a possible pathway for transferring S-MIFs to the CM parent body.

5.4.5. Multiple implications and limitations of ice-based models

The ices are required to have carried H_2S with heterogeneous S isotopic compositions to account for the varying $\Delta^{36}S/\Delta^{33}S$ values observed from sample to sample (Fig. 5). This hypothesis contrasts with the suggestion that the ices carried other isotopically extreme but homogeneous components (Alexander et al., 2015). Naively, a correlation

between water content and S content (or isotopic composition) might be expected in any ice-based model, but they are not observed (Table 1, Table 2). However, some water must have been consumed by metal oxidation (e.g., Wilson et al., 1999, Rosenberg et al., 2001, Alexander et al., 2010, Alexander et al., 2012). It is also possible that sulfides and S^0 were less mobile than water (after the ice melted), and/or that H_2S was mostly in the gas phase and moved independently of the water. Thus, the observed lack of a correlation between water and S is not seen as a weakness of this type of model. Model B-1 requires that the H_2S trapped in ices have S isotope compositions consistent with what is observed for S^0 in experiments (i.e., mainly negative $\Delta^{33}S$ values relative to CDT, Chakraborty et al., 2013), and not with the residual H_2S. This might be a weakness of the model, and experimental studies are needed to establish whether H_2S photodissociation can lead to the formation of S^0 with positive $\Delta^{33}S$ values with $\Delta^{36}S/\Delta^{33}S$ values of around −3. Under the model B-2, the ices would end up hosting both H_2S and S^0 with complementary S-MIFs. Both species would be released upon melting of the ice in the asteroid parent body, and H_2S would be left to react with the iron species in the fluids, leading to the further production of S^0 and sulfides (like in model B-1). However, under the current state of knowledge, the proportion of S^0 provided by the ices, relative to the S^0 formed by reaction 1 (whom the ice H_2S is the precursor), is unknown. If the former were dominant, S^0 and sulfides would have uncorrelated $\Delta^{33}S$ values. If the latter were dominant, S^0 and sulfides would have negatively correlated $\Delta^{33}S$ values. In both cases, the positive correlation between the S^0 and H_2S values (Fig. 6b) would be left unaccounted for, constituting a significant weakness of the model. However, we note that B-2 is not mutually exclusive with B-1. A combination of the two models is possible, and would simply produce some of the scatter observed among the compositions of the S-bearing components of the various CMs.

Finally, H_2S ice irradiation in the presence of CH_3OH has been shown to lead to the formation of S-bearing organic molecules (Jiménez-Escobar et al., 2014, Mahjoub et al., 2016). This is a critical observation, as if the H_2S photodissociation process occurred during the ice-warming events (associated with H_2S sublimation), it could lead to the production of S-MIF (Chakraborty et al., 2013) and its transfer to organic molecules. This mechanism has been explored for the production of C,N-bearing organics by UV irradiation of ice at high altitude in the disk, aided by vertical motions in the protoplanetary nebula (Ciesla and Sandford, 2012). Significant S-MIF has been reported for the soluble organic fraction of Murchison (with $\Delta^{33}S$ values up to +2.00 ± 0.05‰), but their origin remains unclear (Cooper et al., 1997). The model B-2

presented here, combined with the dynamical considerations of Ciesla and Sandford (2012), possibly accounts for these signatures.

5.5. What are the next steps to test the models?

While both models explored here can explain the general features of S isotopic heterogeneity in the CMs, they also both have significant limitations. To test these models, experimental studies are needed to fully describe the gaseous and aqueous S chemistries. For example, to test model A, experimental studies are needed to constrain the condensation behavior of S^0 under canonical nebular conditions, with and without UV light. It is also essential to constrain the reaction rate law of reaction 3, to establish whether S^0 in the vapor phase would back react to H_2S. If not, MIF-bearing sulfide could be directly condensed, even in model B-1, without having the formation of late MIF-carrying sulfides as a requirement. Model B-1, in turn, can be tested through studies of the S^0 chemistry in an aqueous environment and in the presence of H_2. The rates of reactions (1), (2) under the relevant conditions need to be explored in future studies to test our hypothesis. Finally, to constrain the model B-2, it will be critical to address the possibility that H_2S ice irradiation by UV (or protons), described to produce S^0 and S-bearing organics (Jiménez-Escobar and Caro, 2011, Jiménez-Escobar et al., 2014, Moore et al., 2007, Mahjoub et al., 2016), is associated with S-MIF production.
In general, if the anomalous S isotopic compositions in CMs are linked with the accreted ices, predictions can be made for other types of chondrites: The various chondrites parent bodies did not accrete similar amounts of ice (e.g., Clayton and Mayeda, 1999, Alexander et al., 2012). Consequently, they would in principle have distinct S-MIF signatures. For example, COs are similar to CMs in terms of bulk chemical composition (Wasson and Kallemeyn, 1988), although they accreted significantly less matrix (Krot et al., 2009 and references therein). The CO parent body, therefore, presumably accreted significantly less ice than the CMs (Clayton and Mayeda, 1999). If the CMs S isotopic signature is linked with ice accretion only, COs would be predicted to host mass dependant S isotopic signatures.
Finally, we also treated all our data as if the CMs are pristine chondrites that were never subjected to impact processes. These chondrites are, however, breccias (Metzler et al., 1992). It is conceivable that S^0 and sulfides would be redistributed during the brecciation process. In that case, the isotopic relationship between S^0 and sulfides may have been obscured. That could explain why Banten is the only CM studied here that has sulfide with $\Delta^{33}S$ depletion relative to S^0but lies on a $\Delta^{36}S/\Delta^{33}S$ of around −3. Since varying $\Delta^{36}S/\Delta^{33}S$ between different CMs (Murchison and MCY 05230 versus the other CMs)

require some degree of heterogeneous accretion of MIF-bearing sulfides and S^0, an alternative is that a similar process heterogeneously accreted S-bearing phases to Banten.

5.6. Implications for sulfur chemistry in the early solar system

A striking feature of the meteoritic sulfur isotope record is the lack of large mass-dependent and mass-independent isotopic signatures, such as those seen for other elements that partitioned into multiple gas phase molecular species. Spectroscopic observations of multiple S-bearing molecules in molecular clouds (e.g., H_2S, OCS, SO_2, HSCN, CH_2S, CH_3S, C_2H_5S, S_3, C_2S, SO, $HSCS^+$, and SO^+: Müller et al., 2005) suggest a rich photochemistry and ion-molecule chemistry for S in the gas phase. As has already been discussed above, photochemical reactions can produce significant S-MIF (up to +1.5‰). The occurrence of significantly smaller S-MIF in chondrites (this study) and achondrites (Farquhar et al., 2000a, Rai et al., 2005, Rai and Thiemens, 2007, Antonelli et al., 2014) suggests that S may have been homogenized to a significant extent in the nebula. The MIF-S signatures in achondrites have been interpreted to reflect such a processing in high-temperature nebular environments, near the Sun (Rai et al., 2005, Rai and Thiemens, 2007, Chakraborty et al., 2013, Antonelli et al., 2014).

The standard model to explain S-MIF in achondrites is based on the observation of a +0.161 ± 0.012‰ $\Delta^{33}S$ values in Norton County oldhamites (Rai et al., 2005). The assertion is that sulfide such as CaS could be a refractory carrier of isotope anomalies to asteroids (Rai et al., 2005). If the isotopic composition of oldhamite records photo-processed H_2S (Rai et al., 2005), the production of complementary S^0 carrying negative $\Delta^{33}S$ values was required by this observation. This S^0 must also have escaped condensation consistent with its low condensation temperature, and reaction with H_2 back to H_2S (i.e., reaction 3) as it would otherwise lead to the preservation of a CDT-like $\Delta^{33}S$ value in the bulk H_2S and in the condensed sulfides. Later on, the CaS grains could have been transported to various nebular regions where they would have been incorporated into meteorite parent bodies, possibly through X-winds (Rai et al., 2005). H_2S photodissociation cannot occur at the nebular midplane as it is where the optical density is the highest (Ciesla, 2010). It would rather occur close to the sun, where optical density allows UV light to interact with gas phases (Rai et al., 2005, Antonelli et al., 2014). Note that in addition, the reduced conditions closer to the sun (produced by H_2O depletion) are required by the occurrence of refractory Ca,Mg-sulfides as canonical

C/O nebular conditions would otherwise bind calcium and magnesium to oxygen, not sulfur (Lodders, 2003).

Further complications arising with this model are revealed by examination of the oldhamite data from aubrites. Rai et al. (2005) and Defouilloy et al. (2016) report highly variable $\Delta^{33}S$ values for oldhamite separates coming from the Norton County aubrite. In addition, the incorporation of CaS in the aubrite parent body must have occurred late, likely after the aubrite asteroid differentiation, so that anomalous $\Delta^{33}S$ values relative to bulk sulfur could be preserved in refractory sulfides (and not mixed during magmatic processes). This has chronological implications on how the disk produces and distributes early-condensed refractory sulfides to asteroids.

Refractory sulfides do not contribute to our extracted S (Section 3.1). Only the Sutter's Mill CM, that also displays evidence for mixing with enstatite chondrite during brecciation, have been reported to contain oldhamites (Zolensky et al., 2014). CMs only contain Fe-(Ni-)sulfides (and tochilinites), produced by the parent body processing of Fe-sulfides; Fe-sulfides being the principal sulfide phase predicted to form under canonical C/O conditions (Zolensky and Thomas, 1995, Lodders, 2003, Rubin et al., 2007). The direct observation of S^0 carrying most of the $\Delta^{33}S$ variability, and of sulfide carrying complementary $\Delta^{33}S$ values, shows that the condensation of refractory CaS is not required to preserve non-CDT $\Delta^{33}S$ values. In that case, the H_2S photodissociation could occur at the surface of the disk, and provide another way to produce S-MIF. Vertical motion is a natural consequence of realistic disk viscosities (Ciesla, 2010, Ciesla and Sandford, 2012). Over timescales of $<10^5$ years, many particles would have experienced significant UV irradiation simply through vertical motions that transported matter from the midplane to high altitudes in the disk (Ciesla, 2010, Ciesla and Sandford, 2012). We thus suggest the surface of the disk as a viable location for H_2S photodissociation recorded in CMs.

Our observations do not negate the validity of the refractory sulfide model, as these phases are directly observed to carry S-MIF in the aubrite meteoritical record (Rai et al., 2005, Defouilloy et al., 2016). Rather, our dataset establishes the fact that at least two S-MIF producing process were operating in the solar nebula, one producing the refractory sulfides observed in aubrites, and one producing the variations observed in CMs. The expansion of the refractory sulfide model to iron meteorites (Antonelli et al., 2014) may be valid, but our observation offers an alternative mechanism for S photochemistry that can be achieved under canonical C/O conditions, and possibly at any heliocentric distance provided a mechanism exists for preserving and transferring the S-MIF to planetesimals.

A H_2S photodissociation mechanism, similar to the ones described in our model A does not require the involvement of ice accretion (or any subsequent parent body processes) to transfer S-MIF to asteroids, and could then be extended to meteorite precursors formed in the inner region of the solar system like iron meteorites (Bottke et al., 2006). This scenario would lead to the formation of variable $\Delta^{33}S$ values for S^0 and FeS. Any deposited S^0 is likely to have experienced reduction to sulfide during differentiation of the parent bodies of meteorites; this is because parent bodies of all known achondrites and iron meteorites have fO_2 only allowing S^{2-} as the stable S-bearing phase (e.g., Métrich et al., 2009). Thus, the heterogeneous distribution of the photodissociation products and residues (like those observed among the CMs) could easily lead to the ~0.05‰ $\Delta^{33}S$ variations observed in the achondrites and irons (Farquhar et al., 2000a, Antonelli et al., 2014). This process could also be recorded in the chondrule precursors of ordinary chondrite, accounting for the S-MIF observed in some of these objects (Rai and Thiemens, 2007). In addition to relaxing the requirement of a reduced, hot inner nebula for the production and sequestration of S-MIF in the meteorite record, this model eliminates the need for the redistribution of grains formed near the proto-Sun to the achondrite-forming region. Importantly, this removes any requirement for the X-wind model or other disk winds to explain the occurrence of S-MIF in meteorites that form in distal cooler regions of the nebula.

The ice-based models, in turn, could not be expanded to iron meteorite, as these bodies were likely formed too close to the sun to accrete significant amount of ices (Bottke et al., 2006). However, the potential of S-MIF production during ice transport (by UV irradiation of the ices: Jiménez-Escobar and Caro, 2011, Ciesla and Sandford, 2012) could explain the S-MIF observed in the only study of the organic phases of the Murchison meteorite (Cooper et al., 1997). This would relax the hypothesis that interstellar S was involved in meteoritical organic matter (Cooper et al., 1997), and support the idea that UV processing of ices before their accretion to asteroids can be associated with at least a portion of the organic matter present in chondrites (Ciesla and Sandford, 2012).

6. Conclusions

We report the results of measurements of the abundances and the quadruple S isotopic composition of sulfide, sulfate and S^0 in 13 CM carbonaceous chondrites. Our samples include 4 falls and 9 finds, and display an average S content of 2.11 ± 0.39 wt.% S (1σ). The recovered sulfate, S^0 and sulfide contents represent 25 ± 12%, 10 ± 7% and 65 ± 15% of the bulk S, respectively (all 1σ).

We report ranges of S-MIFs in carbonaceous chondrites that are larger than previously observed. The largest variations are captured by S^0, with $\Delta^{33}S$ values ranging between −0.104 ± 0.012‰ (LEW 87022, 2σ) and +0.256 ± 0.018‰ (MCY 05230, 2σ). The $\Delta^{36}S/\Delta^{33}S$ values of S^0 are on average −3.1 ± 1.0 (2σ). When sulfides and sulfates are taken into account, the average $\Delta^{36}S/\Delta^{33}S$ value is −3.9 ± 2.2 (2σ). The only exceptions are MCY 05230 and one of two Murchison samples that have $\Delta^{36}S/\Delta^{33}S$ values of +1.3 ± 0.1 and +0.9 ± 0.1, respectively, for their S^0 (note that their sulfides and sulfates display similar positive $\Delta^{36}S/\Delta^{33}S$ values as well).

Non-zero $\Delta^{33}S$ values are also preserved in sulfide and sulfate, and are correlated with S^0 values. The observed trends suggest a genetic relationship between the extracted S-bearing phases. For sulfate, the $\Delta^{33}S$ trend with S^0 values has a slope of 0.86 ± 0.24 (2σ). This slope is consistent with sulfate was produced by S^0 oxidation, not sulfide oxidation, during parent body processing. For sulfide, the slope of the $\Delta^{33}S$ trend with S^0 is 0.56 ± 0.20(2σ). This suggests that the genetic link between S^0 and sulfide is more complex.

H_2S photodissociation experiments with UV light (wavelength <150 nm) have previously demonstrated the formation of MIF-bearing S^0. The sign of our $\Delta^{33}S$ values, and the $\Delta^{36}S/\Delta^{33}S$ values of our S-bearing extracts are consistent with the experimental data. We have explored two types of models, both requiring H_2S photodissociation, to explain our data. Although imperfect, these models explain the major features of the CM S isotope compositions, and can be tested experimentally in future studies. In model A, sulfides and $S^0$are both condensates produced after incomplete H_2S photodissociation.

A distillation process during photodissociation would account for the sign and range of the S-MIF observed in S^0 and sulfides. This mechanism requires that the product of the photodissociation (S^0) is removed from the system via condensation immediately after its production. It also requires the troilite formation occurs contemporaneously with S^0 condensation. The well-documented rate for metal sulfidation would indicate a temperature window for troilite formation between 500 K and 700 K. Although poorly known, the S^0 condensation temperature inferred from the literature seems too low to allow such process to occur.

In model B-1, H_2S experienced partial photodissociation at $T < 500$ K. Some of this H_2S would be trapped in ices that were later accreted, along with the condensed S^0, by the CMs in their matrices. Melting of the ice in the CM parent body would have released this H_2S, enabling it to react with iron in metal and in solution, leading to the formation of a second generation of sulfides, as well as S^0. These late phases would carry the S-MIF presently observed. This model requires ices to accrete H_2S with heterogeneous S

isotopic compositions. A model B-2 includes the possibility of further photo-processing of H_2S in the ices prior to accretion by the CM parent body.
Our observations offer a mechanism for S photochemistry that can be achieved under canonical C/O conditions, allowing revisiting the origin of S-MIF in other meteorites and relaxing the need for invoking the X-wind model. A H_2S photodissociation mechanism, similar to the ones recorded in CMs, would lead to the formation of variable $\Delta^{33}S$ values in condensed phases, and their heterogeneous distribution could easily lead to the small $\Delta^{33}S$ variations observed in other meteorite groups, including non-chondrites.

Acknowledgements

This work was supported by a Carnegie (Geophysical Laboratory) postdoctoral fellowship granted to JL. JF acknowledges
the NASA Cosmochemistry grant NNX13AL13G. CA was also partially supported by NASA Cosmochemistry grant NNX14AJ54G. For generously supplying the samples, the authors would like to thank: the British National History Museum, the members of the Meteorite Working Group, Cecilia Satterwhite and Kevin Righter (NASA, Johnson Space Center), Tim McCoy, Cari Corrigan and Linda Welzenbach (Smithsonian Institute), and Laurence Garvie (Arizona State University). US Antarctic meteorite samples are recovered by the Antarctic Search for Meteorites (ANSMET) program, which has been funded by NSF and NASA, and characterized and curated by the Department of Mineral Sciences of the Smithsonian Institution and Astromaterials Curation Office at NASA Johnson Space Center. We thank Munir Humayun and three anonymous reviewers for comments that greatly improved this study. We also thank James Dottin and Michael Antonelli for comments on the manuscript. We thank Joost Hoek, Doug Rumble, Anat Shahar, Alan Boss and George Cody for technical help and discussions throughout this study.

Appendix A. Relationships between sulfur extracted at the AVS step, step 12, and step 13

Some details are provided here as to how S extracted during the AVS, step 12 and step 13 are related. In the context of the $\Delta^{33}S$ variability across our CMs, there is a significant match between $\Delta^{33}S$ values of these three pools, suggesting that they are related (see Sections 3.1 Extraction, 5.3 Sulfur cosmochemistry). There are some exceptions to this first order rule. The three samples that display the most negative $\Delta^{33}S$ values for their bulk sulfide (DOM 08013, Banten, and LEW 87022) yield AVS $\Delta^{33}S$ values that are higher than the steps 12 or 13 extracts (Supp Fig. 2). Banten $\Delta^{33}S$ values for steps 12

and 13 are −0.050 ± 0.009‰ and −0.037 ± 0.009‰, respectively, whereas the AVS value is +0.007 ± 0.010‰ (all 2σ). A possible explanation is a contamination of steps 12 and 13 by the naturally occurring S^0 (step 2). This is conceivable if some of the interstitial S^0 was, for some reason, unexposed to solvation during the ethanol extraction, and instead later released during the HCl digestion. This S^0 would be a contaminant for steps 12 and 13, but not for the AVS pool. However, the step 2 $\Delta^{33}S$ values in those chondrites are inconsistent with this hypothesis: For Banten, it is −0.001 ± 0.006‰, which is statistically indistinguishable from AVS but significantly higher than steps 12 and 13. An alternative possibility to explain the observations is to invoke complex sulfide mineralogy. The occurrence of non-FeS sulfides, that would carry a distinct $\Delta^{33}S$, would be required. These sulfides would be extracted during the AVS step without being partially oxidized to S^0 due to their distinct mineralogy. Why such sulfide phases would occur exclusively in the CMs displaying negative $\Delta^{33}S$ is unclear, but exotic sulfide phases are known to occur in some CMs (e.g., Ma et al., 2010) and careful petrographic studies are needed to evaluate whether our working hypothesis to explain these results is valid.

The $\Delta^{33}S$ values of steps 12 or 13 are indistinguishable for all samples (Supp Fig. 2A, Table 3), including the three CMs described above, except LEW 85312 that shows a $\Delta^{33}S$ step 12 value of +0.015 ± 0.005‰ (indistinguishable from its AVS value of +0.010 ± 0.007‰) and a step 13 value of −0.075 ± 0.006‰ (Supp Fig. 2A). For this CM, the step 13 represents ~13,000 ppm S, or 86% of the sulfide, which is typical of the other CMs studied here. Such a distinct isotopic composition remains puzzling. Since the step 12 and AVS isotopic compositions for LEW 85312 are indistinguishable, as are steps 12 and 13 in all the other CMs, it is possible that the LEW 85312 step 13 was contaminated in some way. This CM has a $\Delta^{33}S$ value for step 2 of −0.080 ± 0.020‰ (2σ), indistinguishable from the step 13 value. Because these compositions are so similar, if the LEW 85312 step 13 acquired its isotopic composition through contamination with native S^0 (normally extracted in step 2), it would require that the native S^0 dominate step 13, which seems unlikely. In addition, any S^0 not extracted in step 2 would be partially extracted during the AVS treatment and recovered in step 12 as well, which we see no evidence for.

Appendix B. PCA 91084 represents the specific case of heated CMs

Only one heated CM was studied here. PCA 91084 displays $\Delta^{33}S$ values that are in the range of other CMs. However, the S chemistry in this chondrite displays a slightly distinct pattern. First, the sulfate pool is the dominant S-bearing phase, with

12,935 ± 100 ppm S as sulfate in this CM. Also, the $\delta^{34}S$ composition of sulfate in this CM is +1.65 ± 0.5‰, the highest sulfate value of our samples. Its S^0 $\delta^{34}S$ value is −1.84 ± 0.15‰, the lowest S^0 value across the studied CM, resulting in the only negative $\delta^{34}S_S$–$\delta^{34}S_{sulfate}$ value of −3.5 ± 0.5‰. These data are consistent with a heating process affecting the sulphur chemistry, where sulfates would be produced in larger quantities. Because the $\delta^{34}S$–$\Delta^{33}S$ relationship between sulfate and S^0 is preserved (Fig. 9. PCA 91084 is actually an endmember of this relationship), is likely that this sulfate would be produced by S^0 oxidation. The S^0content of this CM is 3191 ± 100 ppm, i.e. in the higher S content values for this pool. It is possible that sulfide were oxidized to S^0 in large quantities (as observed in LEW 85312), subsequently oxidized to sulfate. The isotope compositions of these pools are consistent with a larger consumption of S^0 to sulfate, or with an attainment of isotope equilibrium (favouring the heavy S isotope in the most oxidized compound) during oxidation. This one CM may reveal the potential of the S systematic to describe the process of heat metamorphismaffecting CMs, and a specific study is clearly needed to discuss the questions outlined here.

Appendix C. Supplementary data

Download Acrobat PDF file (117KB)Help with pdf files

Supplementary data 1. Comparison for the estimates of S^0content in CMs, between Ag_2S weighing and High Performance Liquid Chromatography (HPLC) determination. The samples lie on a 1:1 line, indicating the robustness of our approach.

Download Acrobat PDF file (190KB)Help with pdf files

Supplementary data 2. An evaluation of the genetic links between the AVS, step 12, and step 13 extracts. Shown in red are the 1:1 slopes. The $\Delta^{33}S$ values of (a) step 12 is compared to step 13, (b) AVS is compared to step 12 and (c) step 13. Only LEW 85312 shows distinct $\Delta^{33}S$ step 12 and step 13 values. The AVS extracts of DOM 08013, Banten, and LEW 87022 yield AVS $\Delta^{33}S$ values that are higher than the steps 12 or 13 extracts. Besides those examples, there is an overall first order match between the AVS, step 12 and step 13 $\Delta^{33}S$ values for most meteorites, compared to resolvable $\Delta^{33}S$ difference between CMs, strongly suggesting that S in these three steps was likely derived from the same phases (see Section 5.3).

Download Acrobat PDF file (114KB)Help with pdf files

Supplementary data 3. An evaluation of the genetic links between the naturally occurring elemental S (i.e. step 2) and the elemental sulfur recovered during the sulfide extraction (step 13). There is a positive correlation, but the data are not distributed on a 1:1 slope. We see the positive trend as a reflection of the $\Delta^{33}S$ correlation between sulfide (that are mostly sampled by the step 13 of our protocol) and naturally occurring elemental S, as what is observed on Fig. 7B.

References

Alexander et al., 2007

C.M.O'D. Alexander, M. Fogel, H. Yabuta, G.D. Cody**The origin and evolution of chondrites recorded in the elemental and isotopic compositions of their macromolecular organic matter**

Geochim. Cosmochim. Acta, 71 (2007), pp. 4380-4403

ArticleDownload PDFView Record in Scopus

Alexander et al., 2010

C.M.O'D. Alexander, S.D. Newsome, M.L. Fogel, L.R. Nittler, H. Busemann, G.D. Cody**Deuterium enrichments in chondritic macromolecular material—implications for the origin and evolution of organics, water and asteroids**

Geochim. Cosmochim. Acta, 74 (2010), pp. 4417-4437

ArticleDownload PDFView Record in Scopus

Alexander et al., 2012

C.M.O'D. Alexander, R. Bowden, M.L. Fogel, K.T.Howard, C.D.K. Herd, L.R. Nittler**The provenances of asteroids, and teir contributions to the volatile inventories of the terrestrial planets**

Science, 337 (2012), pp. 721-723

CrossRefView Record in Scopus

Alexander et al., 2013

C.M.O'D. Alexander, K.T. Howard, R. Bowden, M.L.Fogel**The classification of CM and CR chondrites using bulk H, C and N abundances and isotopic compositions**

Geochim. Cosmochim. Acta, 123 (2013), pp. 244-260

ArticleDownload PDFView Record in Scopus

Alexander et al., 2015

C.M.O'D. Alexander, R. Bowden, M.L. Fogel, K.T.Howard**Carbonate abundances and isotopic compositions in chondrites**

Meteorit. Planet. Sci., 50 (2015), pp. 810-833

CrossRefView Record in Scopus

Airieau et al., 2005

S.A. Airieau, J. Farquhar, M.H. Thiemens, L.A. Leshin, H. Bao, E. Young**Planetesimal sulfate and aqueous alteration in CM and CI carbonaceous chondrites**

Geochim. Cosmochim. Acta, 69 (2005), pp. 4167-4172

ArticleDownload PDF

Antonelli et al., 2014

M.A. Antonelli, S.T. Kim, M. Peters, J. Labidi, P.Cartigny, R.J. Walker, J.R. Lyons, J. Hoek, J. Farquhar**Early inner solar system origin for anomalous sulfur isotopes in differentiated protoplanets**

Proc. Natl. Acad. Sci., 111 (2014), pp. 17749-17754

CrossRefView Record in Scopus

Bains-Sahota and Thiemens, 1988

S.K. Bains-Sahota, M.H. Thiemens**Fluorination of SF_4, SF_5Cl, and S_2F_{10} to SF_6 for mass spectrometric isotope ratio analysis**

Anal. Chem., 60 (1988), pp. 1084-1086

CrossRefView Record in Scopus

Baroni et al., 2007

M. Baroni, M.H. Thiemens, R.J. Delmas, J. Savarino**Mass-independent sulfur isotopic compositions in stratospheric volcanic eruptions**

Science, 315 (2007), pp. 84-87

CrossRefView Record in Scopus

Beck et al., 2012

P. Beck, V. De Andrade, F.R. Orthous-Daunay, G.Veronesi, M. Cotte, E. Quirico, B. Schmitt**The redox state of iron in the matrix of CI, CM and metamorphosed CM chondrites by XANES spectroscopy**

Geochim. Cosmochim. Acta, 99 (2012), pp. 305-316

ArticleDownload PDFView Record in Scopus

Benedix et al., 2015

Benedix G. K., Russell S. S., Forman L. V., Bevan A. W. R. and Bland P. A. (2015) A new unequilibrated chondrite lithology discovered in the Murchison CM2 meteorite. In: Lunar Planet. Sci. XLVI. Lunar Planet. Inst., Houston #1143(abstr.).

Bland et al., 2009

P.A. Bland, M.D. Jackson, R.F. Coker, B.A. Cohen, J.B.W. Webber, M.R. Lee, C.M. Duffy, R.J. Ch ater, M.G. Ardakani, D.S. McPhail, D.W. McComb, G.K. Benedix**Why aqueous alteration in asteroids was isochemical: high porosity≠ high permeability**

Earth Planet. Sci. Lett., 287 (2009), pp. 559-568

ArticleDownload PDFView Record in Scopus

Bottke et al., 2006

W.F. Bottke, D. Nesvorný, R.E. Grimm, A. Morbidelli, D.P. O'Brien**Iron meteorites as remnants of planetesimals formed in the terrestrial planet region**

Nature, 439 (2006), pp. 821-824

CrossRefView Record in Scopus

B o u l e

gue, 1978

J. Boulegue**Solubility of elemental sulfur in water at 298 K**
Phosphorus Sulfur Relat. Elem., 5 (1978), pp. 127-128
CrossRefView Record in Scopus

Browning et al., 1996

L.B. Browning, H.Y. McSween, M.E. Zolensky**Correlated alteration effects in CM carbonaceous chondrites**
Geochim. Cosmochim. Acta, 60 (14) (1996), pp. 2621-2633
ArticleDownload PDFView Record in Scopus

Bullock et al., 2005

E.S. Bullock, M. Gounelle, D.S. Lauretta, M.M. Grady, S.S. Russell**Mineralogy and texture of Fe-Ni sulfides in CI1 chondrites: clues to the extent of aqueous alteration on the CI1 parent body**
Geochim. Cosmochim. Acta, 69 (2005), pp. 2687-2700
ArticleDownload PDFView Record in Scopus

Bullock et al., 20

E.S. Bullock, K.D. McKeegan, M. Gounelle, M.M.Grady, S.S. Russell**Sulfur isotopic composition of Fe–Ni sulfide grains in CI and CM carbonaceous chondrites**
Meteorit. Planet. Sci., 45 (2010), pp. 885-898
CrossRefView Record in Scopus

Burgess et al., 1

R. Burgess, I.P. Wright, C.T. Pillinger**Determination of sulphur-bearing components in C1 and C2 carbonaceous chondrites by stepped combustion**
Meteoritics, 26 (1991), pp. 55-64
CrossRefView Record in Scopus

Canfield et al., 1

D.E. Canfield, R. Raiswell, J.T. Westrich, C.M. Reaves, R.A. Berner**The use of chromium reduction in the analysis of reduced inorganic sulfur in sediments and shales**

Chem. Geol., 54 (1986), pp. 149-155
ArticleDownload PDFView Record in Scopus

Chakraborty et a

S. Chakraborty, T.L. Jackson, M. Ahmed, M.H.Thiemens**Sulfur isotopic fractionation in vacuum UV photodissociation of hydrogen sulfide and its potential relevance to meteorite analysis**
Proc. Natl. Acad. Sci., 110 (2013), pp. 17650-17655
CrossRefView Record in Scopus

Ciesla, 2010

F.J. Ciesla**Residence times of particles in diffusive protoplanetary disk environments. I. Vertical motions**
Astrophys. J., 723 (2010), p. 514
CrossRefView Record in Scopus

Ciesla, 2015

F.J. Ciesla**Sulfidization of iron in the dynamic solar nebula and implications for planetary compositions**
Astrophys. J. Lett., 800 (2015), p. L6
CrossRefView Record in Scopus

Ciesla and Sand

F.J. Ciesla, S.A. Sandford**Organic synthesis via irradiation and warming of ice grains in the solar nebula**
Science, 336 (2012), pp. 452-454
CrossRefView Record in Scopus

Clayton and May

R.N. Clayton, T.K. Mayeda**Oxygen isotope studies of achondrites**
Geochim. Cosmochim. Acta, 60 (1996), pp. 1999-2017
ArticleDownload PDFView Record in Scopus

Clayton and May

R.N. Clayton, T.K. Mayeda**Oxygen isotope studies of carbonaceous chondrites**
Geochim. Cosmochim. Acta, 63 (13) (1999), pp. 2089-2104
ArticleDownload PDFView Record in Scopus

Cooper et al., 19

G.W. Cooper, M.H. Thiemens, T.L. Jackson, S. Chang**Sulfur and hydrogen isotope anomalies in meteorite sulfonic acids**
Science, 277 (1997), pp. 1072-1074
CrossRefView Record in Scopus

Craig, 1957

H. Craig**Isotopic standards for carbon and oxygen and correction factors for mass-spectrometric analysis of carbon dioxide**

Geochim. Cosmochim. Acta, 12 (1957), pp. 133-149
ArticleDownload PDFView Record in Scopus

Davidson et al., 2

J. Davidson, H. Busemann, L.R. Nittler, C.M.O'D.Alexander, F.R. Orthous-Daunay, I.A. Franchi, P. Hoppe**Abundances of presolar silicon carbide grains in primitive meteorites determined by NanoSIMS**
Geochim. Cosmochim. Acta, 139 (2014), pp. 248-266
ArticleDownload PDFView Record in Scopus

Defouilloy et al.,

C. Defouilloy, P. Cartigny, N. Assayag, F. Moynier, J.A. Barrat**High-precision sulfur isotope composition of enstatite meteorites and implications of the formation and evolution of their parent bodies**
Geochim. Cosmochim. Acta, 172 (2016), pp. 393-409
ArticleDownload PDFView Record in Scopus

Desch et al., 201

S.J. Desch, M.A. Morris, H.C. Connolly Jr, A.P. Boss**A critical examination of the X-wind model for chondrule and calcium-rich, aluminum-rich inclusion formation and radionuclide production**
Astrophys. J., 725 (2010), p. 692
CrossRefView Record in Scopus

Dreibus et al., 19

G. Dreibus, H. Palme, B. Spettel, J. Zipfel, H. Wänke**Sulfur and selenium in chondritic meteorites**
Meteoritics, 30 (1995), pp. 439-445
CrossRefView Record in Scopus

Eiler et al., 2013

J. Eiler, P. Cartigny, A.E. Hofmann, A. Piasecki**Non-canonical mass laws in equilibrium isotopic fractionations: evidence from the vapor pressure isotope effect of SF_6**
Geochim. Cosmochim. Acta, 107 (2013), pp. 205-219
ArticleDownload PDFView Record in Scopus

Farquhar et al., 2

J. Farquhar, T.L. Jackson, M.H. Thiemens**A ^{33}S enrichment in ureilite meteorites: evidence for a nebular sulfur component**
Geochim. Cosmochim. Acta, 64 (2000), pp. 1819-1825
ArticleDownload PDFView Record in Scopus

Farquhar et al., 2

J. Farquhar, J. Savarino, T.L. Jackson, M.H.Thiemens**Evidence of atmospheric sulphur in the martian regolith from sulphur isotopes in meteorites**
Nature, 404 (2000), pp. 50-52

CrossRefView Record in Scopus

Fitzgerald and Ja

M.J. Fitzgerald, A.L. Jaques**Tibooburra, a new Australian meteorite find, and other carbonaceous chondrites of high petrologic grade**
Meteoritics, 17 (1982), pp. 9-26
CrossRefView Record in Scopus

Fuchs et al., 197

L.H. Fuchs, K.J. Jensen, E.J. Olsen**Mineralogy, mineral-chemistry, and composition of the Murchison C2 meteorite**
Smithson. Contrib. Earth Sci., 10 (1973), p. 39
View Record in Scopus

Fujiya et al., 201

W. Fujiya, P. Hoppe, E. Zinner, M. Pignatari, F. Herwig**Evidence for radiogenic sulfur-32 in type AB presolar silicon carbide grains?**
Astrophys. J. Lett., 776 (2013), p. L29
CrossRef

Franz et al., 201

H.B. Franz, S.T. Kim, J. Farquhar, J.M. Day, R.C.Economos, K.D. McKeegan, A.K. Schmitt, A.J. I rving, J. Hoek, J.Dottin III**Isotopic links between atmospheric chemistry and the deep sulphur cycle on Mars**
Nature, 508 (2014), pp. 364-368
CrossRefView Record in Scopus

Fry et al., 1988

B. Fry, W. Ruf, H. Gest, J.M. Hayes**Sulfur isotope effects associated with oxidation of sulfide by O_2in aqueous solution**
Chem. Geol., 73 (1988), pp. 205-210
ArticleDownload PDFView Record in Scopus

Gao and Thieme

X. Gao, M.H. Thiemens**Isotopic composition and concentration of sulfur in carbonaceous chondrites**
Geochim. Cosmochim. Acta, 57 (1993), pp. 3159-3169
ArticleDownload PDFView Record in Scopus

Gautier et al., 20

D. Gautier, F. Hersant, O. Mousis, J.I. Lunine**Enrichments in volatiles in Jupiter: a new interpretation of the Galileo measurements**
Astrophys. J. Lett., 550 (2001), pp. L227-L230
CrossRefView Record in Scopus

Gounelle and Zo

M. Gounelle, M.E. Zolensky**A terrestrial origin for sulfate veins in CI1 chondrites**

Meteorit. Planet. Sci., 36 (2001), pp. 1321-1329
CrossRefView Record in Scopus

Graham et al., 19

A.L. Graham, K. Yanai, H. Kojima, S. Ikadai**Yamato 81020 and Yamato 82042; two new carbonaceous chondrites from Antarctica**
Meteoritics, 20 (1985), p. 654
View Record in Scopus

Hewins et al., 20

R.H. Hewins, M. Bourot-Denise, B. Zanda, H. Leroux, J.A. Barrat, M. Humayun, C. Gopel, R.C. Greenwood, I.A. Franchi, S. Pont, J.P. Lorand, C. Cournede, J. Gattacceca, P. Rochette, M.Kuga, Y. Marrocchi, B. Marty**The Paris meteorite, the least altered CM chondrite so far**
Geochim. Cosmochim. Acta, 124 (2014), pp. 190-222
ArticleDownload PDFView Record in Scopus

Hoppe et al., 201

P. Hoppe, W. Fujiya, E. Zinner**Sulfur molecule chemistry in supernova ejecta recorded by silicon carbide stardust**
Astrophys. J. Lett., 745 (2012), p. L26
CrossRef

Howard et al., 20

K.T. Howard, C.M.O'D. Alexander, D.L. Schrader, K.A.Dyl**Classification of hydrous meteorites (CR, CM and C2 ungrouped) by phyllosilicate fraction: PSD-XRD modal mineralogy and planetesimal environments**
Geochim. Cosmochim. Acta, 149 (2015), pp. 206-222
ArticleDownload PDFView Record in Scopus

Hulston and Thode, 1965

J.R. Hulston, H.G. Thode**Variations in the S^{33}, S^{34}, and S^{36} contents of meteorites and their relation to chemical and nuclear effects**
J .Geophys. Res., 70 (1965), pp. 3475-3484
CrossRefView Record in Scopus

Huss et al., 2003

G.R. Huss, A.P. Meshik, J.B. Smith, C.M. Hohenberg**Presolar diamond, silicon carbide, and graphite in carbonaceous chondrites: Implications for thermal processing in the solar nebula**
Geochim. Cosmochim. Acta, 67 (24) (2003), pp. 4823-4848
ArticleDownload PDFView Record in Scopus

Jarosewich, 1971

E. Jarosewich**Chemical analysis of the Murchison meteorite**
Meteoritics, 6 (1971), pp. 49-52
CrossRefView Record in Scopus

Jiménez-Escobar and Caro, 2011

A. Jiménez-Escobar, G.M. Caro**Sulfur depletion in dense clouds and circumstellar regions-I. H_2S ice abundance and UV-photochemical reactions in the H_2O-matrix**

astron. astrophys., 536 (2011), p. A91

CrossRefView Record in Scopus

Jiménez-Escobar et al., 2014

A. Jiménez-Escobar, G.M. Caro, Y.J. Chen**Sulphur depletion in dense clouds and circumstellar regions. Organic products made from UV photoprocessing of realistic ice analogs containing H_2S**

Mon. Not. R. Astron. Soc., 443 (1) (2014), pp. 343-354

CrossRefView Record in Scopus

Kamyshny et al., 2009

A. Kamyshny, C.G. Borkenstein, T.G. Ferdelman**Protocol for quantitative detection of elemental sulfur and polysulfide zero-valent sulfur distribution in natural aquatic samples**

Geostand. Geoanal. Res., 33 (2009), pp. 415-435

CrossRefView Record in Scopus

Kaplan and Hulston, 1966

I.R. Kaplan, J.R. Hulston**The isotopic abundance and content of sulfur in meteorites**

Geochim. Cosmochim. Acta, 30 (1966), pp. 479-496

ArticleDownload PDFView Record in Scopus

Keller-Rudek et al., 2013

H. Keller-Rudek, G.K. Moortgat, R. Sander, R.Sörensen**The MPI-Mainz UV/VIS spectral atlas of gaseous molecules of atmospheric interest**

Earth Syst. Sci. Data, 5 (2013), pp. 365-373

CrossRefView Record in Scopus

Kerridge et al., 1979

J.F. Kerridge, J.D. Macdougall, K. Marti**Clues to the origin of sulfide minerals in CI chondrites**

Earth Planet. Sci. Lett., 43 (1979), pp. 359-367

ArticleDownload PDFView Record in Scopus

Kinnunen and Saikkonen, 1983

K.A. Kinnunen, R. Saikkonen**Kivesvaara C2 chondrite: silicate petrography and chemical composition**

Bull. Geol. Soc. Finland, 55 (1983), pp. 35-49

CrossRefView Record in Scopus

Krot et al., 2009

A.N. Krot, Y. Amelin, P. Bland, F.J. Ciesla, J. Connelly, A.M. Davis, G.R. Huss, I.D. Hutcheon, K. Makide, K. Nagashima, L.E. Nyquist, S.S. Russell, E.R.D. Scott, K. Thrane, H. Yurimoto, Q.Z. Yin **Origin and chronology of chondritic components: a review**

Geochim. Cosmochim. Acta, 73 (2009), pp. 4963-4997

ArticleDownload PDFView Record in Scopus

Labidi et al., 2012

J. Labidi, P. Cartigny, J.L. Birck, N. Assayag, J.J.Bourrand**Determination of multiple sulfur isotopes in glasses: a reappraisal of the MORB $\delta^{34}S$**

Chem. Geol., 334 (2012), pp. 189-198

ArticleDownload PDF

Labidi et al., 2013

J. Labidi, P. Cartigny, M. Moreira**Non-chondritic sulphur isotope composition of the terrestrial mantle**

Nature, 501 (2013), pp. 208-211

CrossRefView Record in Scopus

Lauretta et al., 1996

D.S. Lauretta, D.T. Kremser, B. Fegley Jr.**The rate of iron sulfide formation in the solar nebula**

Icarus, 122 (1996), pp. 288-315

ArticleDownload PDFView Record in Scopus

Lauretta et al., 1997

D.S. Lauretta, K. Lodders, B. Fegley**Experimental simulations of sulfide formation in the solar nebula**

Science, 277 (1997), pp. 358-360

CrossRefView Record in Scopus

Lewis and Krouse, 1968

J.S. Lewis, H.R. Krouse**Isotopic composition of sulfur and sulfate produced by oxidation of FeS**

Earth Planet. Sci. Lett., 5 (1968), pp. 425-428

ArticleDownload PDFView Record in Scopus

Llorca and Casanova, 2000

J. Llorca, I. Casanova**Reaction between H_2, CO, and H_2S over Fe, Ni metal in the solar nebula: Experimental evidence for the formation of sulfur-bearing organic molecules and sulfides**

Meteorit. Planet. Sci., 35 (4) (2000), pp. 841-848

CrossRefView Record in Scopus

Lodders, 2003

K. Lodders**Solar system abundances and condensation temperatures of the elements**

Astrophys. J., 591 (2003), p. 1220

CrossRefView Record in Scopus

Ma et al., 2010

C. Ma, J.R. Beckett, G.R. Rossman**Discovery of a new chromium sulfide mineral, Cr_5S_6 in Murchison**

Meteorit. Planet. Sci., 45 (2010), p. A124

View Record in Scopus

Mahjoub et al., 2016

A. Mahjoub, M.J. Poston, K.P. Hand, M.E. Brown, R.Hodyss, J. Blacksberg, J.M. Eiler, R.W. Carlo n, B.L. Ehlmann, M.Choukroun**Electron irradiation and thermal processing of mixed-ices of potential relevance to jupiter trojan asteroids**

Astrophys. J., 820 (2016), p. 141

CrossRef

Marrocchi and Libourel, 2013

Y. Marrocchi, G. Libourel**Sulfur and sulfides in chondrules**

Geochim. Cosmochim. Acta, 119 (2013), pp. 117-136

ArticleDownload PDFView Record in Scopus

Mason, 1963

B. Mason**The carbonaceous chondrites**

Space Sci. Rev., 1 (1963), pp. 621-646

CrossRefView Record in Scopus

Matsuhisa et al., 1978

Y. Matsuhisa, J.R. Goldsmith, R.N. Clayton**Mechanisms of hydrothermal crystallization of quartz at 250 °C and 15 kbar**

Geochim. Cosmochim. Acta, 42 (1978), pp. 173-182

ArticleDownload PDFView Record in Scopus

Meyer, 1976

B. Meyer**Elemental sulfur**

Chem. Rev., 76 (3) (1976), pp. 367-388

CrossRefView Record in Scopus

Mayer and Krouse, 2004

B. Mayer, H.R. Krouse**Procedures for sulfur isotope abundance studies**

P.A. de Groot (Ed.), Handbook of Stable Isotope Analytical Techniques, vol. 1, Elsevier, Amsterdam (2004), pp. 538-603

(Chapter 26)

View Record in Scopus

Métrich et al., 2009

N. Métrich, A.J. Berry, H.S.C. O'Neill, J. Susini**The oxidation state of sulfur in synthetic and natural glasses determined by X-ray absorption spectroscopy**

Geochim. Cosmochim. Acta, 73 (2009), pp. 2382-2399

ArticleDownload PDFView Record in Scopus

Metzler et al., 1992

K. Metzler, A. Bischoff, D. Stöffler**Accretionary dust mantles in CM chondrites: evidence for solar nebula processes**

Geochim. Cosmochim. Acta, 56 (1992), pp. 2873-2897

ArticleDownload PDFView Record in Scopus

Moore et al., 2007

M.H. Moore, R.L. Hudson, R.W. Carlson**The radiolysis of SO_2 and H_2S in water ice: Implications for the icy jovian satellites**

Icarus, 189 (2) (2007), pp. 409-423

ArticleDownload PDFView Record in Scopus

Monster et al., 1965

J. Monster, E. Anders, H.G. Thode**$^{34}S/^{32}S$ ratios for the different forms of sulphur in the Orgueil meteorite and their mode of formation**

Geochim. Cosmochim. Acta, 29 (1965), pp. 773-779

ArticleDownload PDFView Record in Scopus

Müller et al., 2005

H.S. Müller, F. Schlöder, J. Stutzki, G. Winnewisser**The Cologne Database for Molecular Spectroscopy, CDMS: a useful tool for astronomers and spectroscopists**

J. Mol. Struct., 742 (2005), pp. 215-227

ArticleDownload PDFView Record in Scopus

Oduro et al., 2011

H. Oduro, B. Harms, H.O. Sintim, A.J. Kaufman, G.Cody, J. Farquhar**Evidence of magnetic isotope effects during thermochemical sulfate reduction**

Proc. Natl. Acad. Sci., 108 (43) (2011), pp. 17635-17638

CrossRefView Record in Scopus

Okabe, 1978

H. Okabe

Photochemistry of small molecules, Vol. 431, Wiley, New York(1978)

Ono et al., 2006

S. Ono, B. Wing, D. Rumble, J. Farquhar**High precision analysis of all four stable isotopes of sulfur (^{32}S, ^{33}S, ^{34}S and ^{36}S) at nanomole levels using a laser fluorination isotope-ratio-monitoring gas chromatography–mass spectrometry**

Chem. Geol., 225 (2006), pp. 30-39

ArticleDownload PDFView Record in Scopus

Pasek et al., 2005

M.A. Pasek, J.A. Milsom, F.J. Ciesla, D.S. Lauretta, C.M.Sharp, J.I. Lunine**Sulfur chemistry with time-varying oxygen abundance during Solar System formation**

Icarus, 175 (2005), pp. 1-14

ArticleDownload PDFView Record in Scopus

Pignatari et al., 2013

M. Pignatari, E. Zinner, M.G. Bertolli, R. Trappitsch, P.Hoppe, T. Rauscher, C. Fryer, F. Herwig, R. Hirschi, F.X. Timmes, F.K. Thielemann**Silicon carbide grains of type c provide evidence for the production of the unstable isotope ^{32}Si in supernovae**
Astrophys. J. Lett., 771 (2013), p. L7
CrossRef

Pruden and Bloomfield, 1968
G. Pruden, C. Bloomfield**The determination of iron (II) sulphide in soil in the presence of iron (III) oxide**
Analyst, 93 (1968), pp. 532-534
CrossRefView Record in Scopus

Rai et al., 2005
V.K. Rai, T.L. Jackson, M.H. Thiemens**Photochemical mass-independent sulfur isotopes in achondritic meteorites**
Science, 309 (2005), pp. 1062-1065
CrossRefView Record in Scopus

Rai and Thiemens, 2007
V.K. Rai, M.H. Thiemens**Mass independently fractionated sulfur components in chondrites**
Geochim. Cosmochim. Acta, 71 (2007), pp. 1341-1354
ArticleDownload PDFView Record in Scopus

Rees and Thode, 1977
C.E. Rees, H.G. Thode**A ^{33}S anomaly in the Allende meteorite**
Geochim. Cosmochim. Acta, 41 (1977), pp. 1679-1682
ArticleDownload PDFView Record in Scopus

Rice et al., 1993
C.A. Rice, M.L. Tuttle, R.L. Reynolds**The analysis of forms of sulfur in ancient sediments and sedimentary rocks: comments and cautions**
Chem. Geol., 107 (1993), pp. 83-95
ArticleDownload PDFView Record in Scopus

Rosenberg et al., 2001
N.D. Rosenberg, L. Browning, W.L. Bourcier**Modeling aqueous alteration of CM carbonaceous chondrites**
Meteorit. Planet. Sci., 36 (2001), pp. 239-244
CrossRefView Record in Scopus

Rubin et al., 2007
A.E. Rubin, J.M. Trigo-Rodríguez, H. Huber, J.T. Wasson**Progressive aqueous alteration of CM carbonaceous chondrites**
Geochim. Cosmochim. Acta, 71 (2007), pp. 2361-2382
ArticleDownload PDFView Record in Scopus

Rumble et al., 1993

D. Rumble, T.C. Hoering, J.M. Palin**Preparation of SF_6 for sulfur isotope analysis by laser heating sulfide minerals in the presence of F_2 gas**
Geochim. Cosmochim. Acta, 57 (1993), pp. 4499-4512
ArticleDownload PDFView Record in Scopus

Shu et al., 1997

F.H. Shu, H. Shang, A.E. Glassgold, T. Lee**X-rays and fluctuating X-winds from protostars**
Science, 277 (1997), pp. 1475-1479
CrossRefView Record in Scopus

Shu et al., 2001

F.H. Shu, H. Shang, M. Gounelle, A.E. Glassgold, T. Lee**The origin of chondrules and refractory inclusions in chondritic meteorites**
Astrophys. J., 548 (2001), p. 1029
CrossRefView Record in Scopus

Simon et al., 2007

S.B. Simon, S.R. Sutton, L. Grossman**Valence of titanium and vanadium in pyroxene in refractory inclusion interiors and rims**
Geochim. Cosmochim. Acta, 71 (2007), pp. 3098-3118
ArticleDownload PDFView Record in Scopus

Sutton et al., 2013

Sutton S., Cloutis E. A. and Alexander C. M. O'D. (2013). The valence state of fe and the origin of water in chondrites. In:Lunar Planet. Sci. XLIV. Lunar Planet. Inst., Houston #2357(abstr.).

Tachibana and Huss, 2005

S. Tachibana, G.R. Huss**Sulfur isotope composition of putative primary troilite in chondrules from Bishunpur and Semarkona**
Geochim. Cosmochim. Acta, 69 (2005), pp. 3075-3097
ArticleDownload PDFView Record in Scopus

Thode et al., 1961

H.G. Thode, J. Monster, H.B. Dunford**Sulphur isotope geochemistry**
Geochim. Cosmochim. Acta, 25 (1961), pp. 159-174
ArticleDownload PDFView Record in Scopus

Wasson and Kallemeyn, 1988

J.T. Wasson, G.W. Kallemeyn**Compositions of chondrites. Philosophical Transactions of the Royal Society of London A: Mathematical**
Phys. Eng. Sci., 325 (1587) (1988), pp. 535-544
CrossRefView Record in Scopus

Wing and Farquhar, 2015

B.A. Wing, J. Farquhar**Sulfur isotope homogeneity of lunar mare basalts**
Geochim. Cosmochim. Acta, 170 (2015), pp. 266-280
ArticleDownload PDFView Record in Scopus

Wilson et al., 1999

L. Wilson, K. Keil, L.B. Browning, A.N. Krot, W. Bourcier**Early aqueous alteration, explosive disruption, and reprocessing of asteroids**

Meteorit. Planet. Sci., 34 (1999), pp. 541-557

CrossRefView Record in Scopus

Young et al., 2002

E.D. Young, A. Galy, H. Nagahara**Kinetic and equilibrium mass-dependent isotope fractionation laws in nature and their geochemical and cosmochemical significance**

Geochim. Cosmochim. Acta, 66 (2002), pp. 1095-1104

ArticleDownload PDFView Record in Scopus

Zahnle and Walker, 1982

K.J. Zahnle, J.C. Walker**The evolution of solar ultraviolet luminosity**

Rev. Geophys., 20 (1982), pp. 280-292

CrossRefView Record in Scopus

Zolensky et al., 1989

M.E. Zolensky, W.L. Bourcier, J.L. Gooding**Aqueous alteration on the hydrous asteroids: results of EQ3/6 computer simulations**

Icarus, 78 (1989), pp. 411-425

ArticleDownload PDFView Record in Scopus

Zolensky and Thomas, 1995

M.E. Zolensky, K.L. Thomas**Iron and iron-nickel sulfides in chondritic interplanetary dust particles**

Geochim. Cosmochim. Acta, 59 (1995), pp. 4707-4712

ArticleDownload PDFView Record in Scopus

Zolensky et al., 1997

M.E. Zolensky, D.W. Mittlefehldt, M.E. Lipschutz, M.S.Wang, R.N. Clayton, T.K. Mayeda, M.M. Grady, C. Pillinger, B.David**CM chondrites exhibit the complete petrologic range from type 2 to 1**

Geochim. Cosmochim. Acta, 61 (1997), pp. 5099-5115

ArticleDownload PDFView Record in Scopus

Zolensky et al., 2014

M. Zolensky, T. Mikouchi, M. Fries, R. Bodnar, P.Jenniskens, Q.Z. Yin, K. Hagiya, K. Ohsumi, M. Komatsu, M.Colbert, R. Hanna, J. Maisano, R. Ketcham, Y. Kebukawa, T.Nakamura, M. Matsuoka, S. Sasaki, A. Tsuchiyama, M. Gounelle, L.Le, J. Martinez, K. Ross, Z. Rahman**Mineralogy and petrography of C asteroid regolith: The Sutter's Mill CM meteorite**

Meteorit. Planet. Sci., 49 (2014), pp. 1997-2016